SEMMELWEIS EGYETEM

DOKTORI ISKOLA

Ph.D. értekezések

2988.

SUHAI FERENC IMRE

Szív- és érrendszeri betegségek élettana és klinikuma
című program

Programvezető: Dr. Merkely Béla, egyetemi tanár

Témavezető: Dr. Szilveszter Bálint, adjunktus

The clinical value of CT angiography and brain MRI following transcatheter aortic valve implantation

PhD thesis

Ferenc Imre Suhai

Doctoral School of Theoretical and Translational Medicine

Supervisor: Bálint Szilveszter, MD, Ph.D

Official reviewers: Sándor Nardai, MD, Ph.D

Eszter Végh, MD, Ph.D

Head of the Final Examination Committee: Tivadar Tulassay, MD, D.sc

Members of the Final Examination Committee: Charaf Hassan, D.sc

Henriette Farkas, MD, D.sc

Budapest

2023

Table of Contents

List of Abbreviations

ACE- Addenbrooke's cognitive assessment

ACE-I Angiotensin-converting-enzyme inhibitor

AD- Axial diffusivity

AF- Atrial fibrillation

AMI- Acute myocardial infarction

ARB- Angiotensin II receptor blockers

AS- Aortic stenosis

AVCS- Aortic valve calcium score

BAV- Bicuspid aortic valve

BMI- Body mass index

BSA- Body surface area

CABG- Coronary artery bypass graft

CC- Corpus callosum

CG- Cingulate gyrus

CHA2DS2-VASc: Congestive heart failure, Hypertension, Age, Diabetes, Stroke/TIA and VAScular disease score

CT- Computed tomography

CTA- Computed tomography angiography

CVE- Cerebrovascular events

DWI- Diffusion-weighted imaging

DTI- Diffusion tensor imaging

FA- Fractional anisotropy

HALT- Hypo-attenuated leaflet thickening

mmHg- Millimetre of mercury

IBL- Ischemic brain lesion

ILV- Ischemic lesion volume

FLAIR- Fluid attenuated inversion recovery

kV- Kilovolt

LA- Left atrium

LV- Left ventricle

LVH- Left ventricular hypertrophy

LVM- Left ventricular mass

MD- Mean diffusivity

MRI- Magnetic resonance imaging

MMSE- Mini-mental state examination

NOAC- Novel oral anticoagulant

NYHA: New York Heart Association functional classification

PAD- Periferial artery disease

PHC- Parahippocampal cingulum

OR- Odds ratio

PCI- Percutaneous coronary intervention

RA- Right atrium

RD- Radial diffusivity

ROI- Region of interest

RV- Right ventricle

SAVR- Surgical aortic valve replacement

SCIL- Silent cerebral ischemic lesion

SD- Standard deviation

SLT- Subclinical leaflet thrombosis

TIA- Transient ischemic attack

TAVI- Transcatheter aortic valve implantation

TC- Transcarotid

TF- Transfemoral

TS- Transsubclavian

TEE- Transesophageal echocardiography

TTE- Transthoracal echocardiography

VARC- Valve Academic Research Consortium

WM- White matter

6M- 6-month follow-up

1Y- One-year follow-up

1. Introduction

Aortic stenosis (AS) is the most common valvular disease in developed countries (1, 2). Its prevalence significantly rises with increasing age and AS has a significant impact on both morbidity and mortality (3). Currently, the standard treatment for patients with severe AS is surgical aortic valve replacement (SAVR). However, transcatheter aortic valve implantation (TAVI) has emerged as a safe and effective alternative to SAVR in symptomatic patients with high or prohibitive risk and as a valid alternative to SAVR in patients with intermediate risk (4-9). TAVI has been recently expanded to lower risk patient population. According to the 2020 US guideline TAVI can be considered for symptomatic patients between the ages of 65 and 80 years, and in asymptomatic patients below 80 years of age with an ejection fraction less than 50% (10, 11). It has been shown, that medical therapy and ballon valvuloplasty is inferior to TAVI in patients who are not suitable for open-heart surgery (12, 13). Moreover, TAVI could potentiate reverse the remodelling of the left ventricle (14) resulting in improved cardiac function and better outcomes (15). As the indication for TAVI expands to lower-risk populations, it becomes increasingly important to consider the prognostic role of left ventricular remodelling and cerebrovascular events (CVE) in patients undergoing this procedure. With the potential for more patients to undergo TAVI, it is crucial to carefully evaluate the impact of the procedure on left ventricular reverse remodelling and the incidence of cerebrovascular events and effect on long term cognitive function which could have a significant impact on short and long-term morbidity and mortality. Therefore, understanding the prognostic significance of these factors will be essential in ensuring the continued success and safety of TAVI in lower-risk patient populations.

1.1. Left ventricular remodelling

AS leads to adaptational adverse cardiac remodelling due to chronic pressure overload of the LV (3). Left ventricular hypertrophy (LVH) is strongly associated with significant risk of cardiovascular mortality and morbidity regardless of its etiology (4, 5). Moreover, chronic pressure overload and subsequent remodelling are accompanied by diastolic and/or systolic LV dysfunction (6-9). LV reverse remodelling will occur immediately after the elimination of afterload (after surgical or transcatheter valve replacement), which means immediate improvement of cardiac function occurs, followed by benefitial reverse

remodelling (LV mass regression) at medium- and long-term. According to the literature, the regression of LV mass (LVM) is a protective factor (15) and is associated with reduced hospitalization rate (16, 17).

1.2. Hypo-attenuated leaflet thickening

Hypo-attenuated leaflet thickening (HALT) of transcatheter aortic valve leaflets has been described on cardiac computed tomography angiography (CTA) datasets in patients after TAVI (18-20). HALT is considered an early imaging feature of subclinical leaflet thrombosis (SLT), which is a common finding after TAVI, the reported frequencies varying from 0.6% to 40% (19, 21). Patients with HALT are mostly asymptomatic, do not exhibit increased transvalvular gradients on echocardiography, and have overt prosthetic valve thrombosis infrequently. HALT can develop despite established post-procedural antiplatelet regimens and, in many cases, may resolve completely after the initiation of anticoagulation therapy. A previous study suggested that valve thickening or thrombosis is considered to have a significant impact on hemodynamic prosthetic valve deterioration (22), which has been linked with less LV reverse remodelling after aortic valve replacement (23). However, whether HALT affects LV reverse remodelling after TAVI and the clinical relevance of SLT is still under debate, some studies find increased risk for stroke or transient ischemic attack (TIA) (18, 24-26), whereas others did not find any associations between SLT and CVE (27-30).

1.3. Cerebral embolization and cerebrovascular events

Cerebrovascular events after TAVI are among the most devastating complications with elevated risk of morbidity and mortality in both the short and long term. (31-33). There is a large variety in defining CVE in prior studies and meta-analyses. The incidence of CVE after TAVI ranges from 1-11%, albeit it was found thast the incidence of periprocedural stroke is slightly higher in patients with first generation transcatheter valves compared to the new generation devices (33-36). According to the Partner 3 trial -which was aimed to investigate whether TAVI could be considered a suitable alternative to SAVR in patients with low surgical risk in patients with severe symptomatic AS- showed a significant reduction in the primary endpoint (composite of death from any cause or disabling stroke) demonstrating superiority against SAVR in this low risk group

(37). The Partner 3 trial reported 3.0% rate of stroke in the TAVI group, and 7.0% in the SAVR group at 30 days. The results of Partner 3 were further strengthened by the publication of the Evolut trial which found that TAVI was non-inferior to SAVR for the primary composite endpoint of death from any cause or disabling stroke at 24 months The Evolut trial found 3.4% rate of stroke in both the TAVI and the SAVR group at 30 days (38).

Besides the clinically apparent ischemic brain lesions, numerous cerebral magnetic resonance imaging (MRI) studies have found a very high (58-91%) incidence of clinically silent new ischemic lesions after TAVI, regardless of the transcatheter valve type and approach (39-42). Although the majority of these lesions did not manifest as an overt stroke, and presents only in a small proportion of patients, silent cerebral embolism is a common finding associated with this procedure. These silent cerebral ischemic lesions (SCIL) might led to impaired cognitive function and the development of future cerebral complications, but the clinical relevance of SCILs is still controversial (43-45). It has been suggested that SCILs after TAVI are associated with increased risk of dementia, cognitive decline and depression (44, 46-48). However, a recently published subgroup analysis from a meta-analysis showed that despite of new cerebral lesions after TAVI, there is a cognitive improvement in 19% and impairment in only 7% of the subjects (49). Also, an inverse correlation was found between low pre-TAVI cognitive performance and post-TAVI cognitive improvement. TAVI could affect cognitive function in either way. The treatment of severe AS by TAVI could improve systolic and diastolic LV function, cerebral perfusion and cognition (50). Nonetheless, it has to be underlined that these fragile patient cohorts have several cerebrovascular risk factors, which might commit to their ischemic brain injury (51). Therefore, state-of-the-art cardiovascular imaging aims to provide accurate assessment of bioprosthetic valve degeneration and provides a possible target for intervention (HALT) and allows for the evaluation of reverse remodelling processes.

1.4. CT angiography (CTA)

CT angiography is a non-invasive modality for the assessment of cardiac function and anatomy, and has a well-defined role in the guidelines for the planning of TAVI procedure (52). CTA is also increasingly used to detect structural valve abnormalities following

TAVI (25, 53-55). To date, most studies evaluating valve function and LV reverse remodelling after TAVI using traditional 2D-echocardiography. Nonetheless, this modality is limited by intra- and interobserver variability and utilizes geometrical assumptions for the calculation of left ventricular mass (LVM), which represents an important source of error in LVM quantification. Due to its exceptional spatial resolution, CTA is a powerful tool that permits accurate LVM assessment with good intra- and interobserver variability and 3-dimensional evaluation of the cardiac chambers (56). LVM evaluated by CTA has really good correlation to the clinical standard method, cardiac magnetic resonance imaging (57). In addition, neither 2D nor 3D transthoracic or transoesophageal echocardiography can directly visualize subclinical leaflet thrombosis (25, 58, 59), which can be depicted using CTA (14). Therefore, in clinical routine, CTA is the method of choice to evaluate HALT and SLT.

1.5. Diffusion MRI

Diffusion weighted imaging (DWI) describes three-dimensional (3-D) diffusion of water molecules, and provides image contrast based on differences in the magnitude of water molecule diffusion within tissues. Diffusion tensor imaging (DTI) is another interpretation method of diffusion MRI data, a promising non-invasive tool for assessment of white matter (WM) connectivity, integrity. widely used to demonstrate microstructural changes in variety of diseases (stroke, schizophrenia, Alzheimer's disease, etc.). This method is also a helpful tool to assess WM changes following TAVI. The diffusion tensor is a 3×3 real, symmetric matrix representation of the three-dimensional water displacement probability in tissue, and it can be represented as an ellipsoid with 3 main axes (51, 59). The length of the longest half-axis reflects diffusion parallel to the supposed WM fibres, i.e. axial diffusivity (AD), the averaged lengths of the two shorter half-axes represent diffusivity perpendicular to the fibres; radial diffusivity (RD) (59, 60, 61). Fractional anisotropy (FA) is a measure of the directionality of diffusion within a voxel. FA value ranges between 0 (isotropic diffusion) and 1 (perfectly anisotropic diffusion). An FA value of 0 means unrestricted diffusion in all directions, 1 means that diffusion occurs along one axis only and is fully restricted along all other directions (62). FA is the highest in compact fibre bundles oriented parallelly, such as the corpus callosum. Whereas myelin damage alone is associated with increased

RD, subacute and chronic axonal damage with a combined myelin injury is shown to result in an increase in AD relative to RD and a decreased FA (59, 63, 64). Decrease in FA is linked with loss of fibre integrity (65) and is observed in age-related WM changes (66, 67) and various diseases (68). Mean diffusivity (MD) is the mean of the three ellipsoid half-axis lengths. MD reflects the magnitude of water diffusion and is proportional to the extracellular water content within a voxel, mainly used for detection of acute brain ischaemia (51). Increased of diffusivity values (MD, AD, RD) can be observed during ageing (66, 69), in mild cognitive impairment (70), in Alzheimer's disease (71), in Parkinson's disease related cognitive impairment (72), and multiple sclerosis (73). DTI might emerge as an useful technique to assess and quantify WM microstructural changes after TAVI.

2. Objectives

2.1. To investigate independent predictors of reverse remodelling after TAVI and to assess the prognostic value of LV reverse remodelling on mortality and hospitalisation for heart failure.

2.2. To assess independent predictors of cerebral embolization after TAVI, and to assess the neurological consequences

- To define independent predictors of patient and procedural related predictors of ischemic lesion volume and stroke

- To evaluate the occurrence and distribution of ischemic brain lesions using diffusion MRI

- To assess the effect of SCILs on the patient's neurocognitive function.

2.3 To assess WM microstructural alterations between the discharge and 6 months brain MRI following TAVI

- To assess DTI metric changes in the corpus callosum and cingulum,

- To correlate DTI metrics with postprocedural ischemic lesion volume (ILV) and evaluate the cognitive trajectory of subjects undergoing TAVI.

3. Methods

3.1. Study population and design

3.1.1. Study population and design for the evaluation of reverse remodelling after TAVI

In a single center, prospective cohort study we analysed 117 consecutive patients who underwent CT angiography for pre-TAVI planning and were assessed following TAVI to determine the presence or absence of SLT as part of the RETORIC study (Rule out Transcatheter Aortic Valve Thrombosis with Post Implantation Computed Tomography trial, NCT02826200) (74). We excluded patients for whom CTA was contraindicated per institutional standard of care (history of severe and/or anaphylactic reaction, severe renal insufficiency defined as ≤30 mL/min/1.73m^2), or who had poor image quality for the evaluation of LVM. As part of the standard clinical evaluation, pre-TAVI imaging was conducted to assess the aortic root anatomy and determine the appropriate access routes (iliofemoral and supraaortic arteries) for transcatheter heart valve sizing and TAVI eligibility. CTA imaging was also utilized to evaluate bioprosthetic valve function and LV morphology after TAVI. All patients received a self-expandable transcatheter aortic valve. Follow-up echocardiography was performed on the same day to to assess LV morphology at various time points following TAVI (average of 1.7 years). Patients with contraindications to CTA per institutional standards of care (such as a history of severe and/or anaphylactic reaction, severe renal insufficiency defined as ≤30 mL/min/1.73m^2) or those with inadequate image quality for assessing left ventricular mass were excluded from the study (14).

3.1.2. Study population and design for the evaluation of procedural predictors of CVE and neurological consequences following TAVI

In a single-center, prospective cohort study, from 153 patients we analyzed 113 consecutive patients after exclusion (consent withdrawal in 6 cases, pacemaker implantation in 19 cases, lack of cooperation in 15 cases) who underwent CT angiography for pre-TAVI planning and brain MRI following TAVI and at six-month (6M) as part of the RETORIC study (29). The valve implantations were performed between November 2016 and June 2018, and patients were followed up until 1 year.

3.1.3. Study population and design for DTI metric and microstructural WM changes

As a part of the previous study, we included subjects into the DTI substudy with complete and adequate discharge TAVI and 6M follow-up MRI datasets. The final DTI study cohort consisted of 78 participants. Inclusion criterion of the cognitive study was the accomplishment of the pre-TAVI baseline and at least one of the three further neurocognitive tests (divided into "DTI cognitive" and "non-DTI cognitive" cohorts) (51).

Written informed consent was obtained from all patients for all of the above described studies. These studies were approved by the local and national ethical committees and were performed in accordance with the Helsinki declaration.

3.2. Image acquisition for TAVI planning and follow-up

We used the following CTA protocol for every pre-TAVI planning CT: first, we acquired a prospectively ECG triggered non-contrast scan from the entire heart (120 kV, slice thickness of 3 mm, increment 1.5 mm). This was followed by a retrospectively ECG-gated CTA of the aorta (from the level of thoracic inlet to the level of the femoral head), and the heart, during a single breath-hold, using a 256-slice CT scanner (Philips Healthcare, 270 msec rotation time, tube voltage of 100-120 kV based on body mass index) for TAVI planning. We administered 75 ml contrast agent with 4.5 ml/s flow, and images were acquired with 1 mm slice thickness, and 1 mm increment using iterative reconstruction (iDose[4] and IMR, Philips Healthcare). Follow-up CT examinations were performed using retrospective gating with similar scan protocol, with shorter scan length covering the volume of the heart and the ascending aorta. CTA was performed in all patients—who did not have contraindication—irrespective of symptoms or echocardiographic results (14).

3.3. Cardiac CTA image analysis

Two radiologists assessed the calcification of aortic valve, annulus, left ventricular outflow tract, ascending aorta and aortic arch on the planning CTA. The severity of calcification was qualitatively graded as mild, moderate, severe. Aortic valve calcium score (AVCS) was measured on the non-contrast cardiac CT, by the Agatston method (Figure 1), with care taken to exclude calcium originating from extravalvular structures (75). LVM was measured at the baseline pre-TAVI and at the follow-up on CTA images in the end-systolic or end-diastolic phases. Semi-automated software tool (Heartbeat-CS, Philips Intellispace v6.0.4) was used for both assessments. For the LVM assessment first, the software segmented the heart and created a short-axis stack through the LV. We adjusted the epi- and endocardial contours manually if needed. The software automatically calculated LVM based on volumetric analysis. The calculated LVM value was indexed to the patients' body surface area. LV reverse remodelling was defined as a reduction of >20% in calculated LVM and LVM index detected on post-TAVI CT scans as compared with pre-TAVI CT scans. The measurements were performed in a random
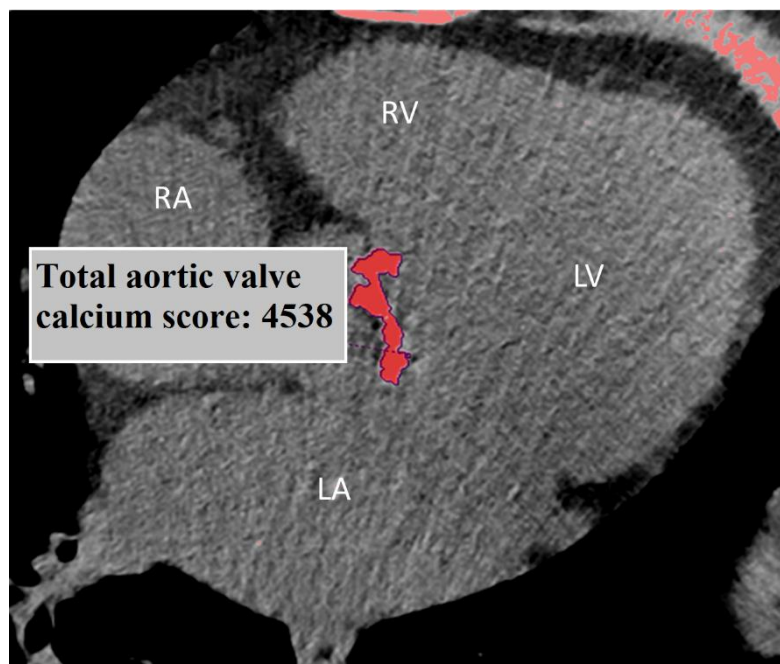
order and investigators were blinded to the scan date and patient data (14).

Figure 1. Non-enhanced CT of severe aortic valve calcification (total AVCS: 4538). Calcium scoring of the aortic valve using post-processing software by the Agatston

method. RA, right atrium; RV, right ventricle; LA, left atrium; LV, left ventricle. Image by the author.

The presence of SLT was evaluated on follow-up CT (average 1.7 years) by three radiologists with at least 5 years of experience in cardiac CT imaging. All readers were blinded to echocardiographic or clinical parameters and assessed SLT within the bioprosthetic valve in the end-diastolic phase. All cusps were evaluated separately for the presence of leaflet thrombosis and the number of involved cusps was recorded. The images were assessed by all three readers as part of a consensus read. In long-axis view the thickness of each leaflet was measured in parallel and perpendicular axes to the frame. An average thickness of >3 mm of the hypo-attenuated mass (based on both the parallel and the perpendicular axis measurements) was considered as leaflet thickening corresponding to SLT (Figure 2) (14).

Figure 2. Representative cases for the assessment of reverse remodelling and SLT. CTA images were analysed to quantify LVM using a semi-automated software. Valve assessment was performed by three radiologists on the follow-up images. LVM was measured on pre- and post-TAVI images to calculate change in LVM (ΔLVM). Case 1 (upper panels) depicts a patient without SLT and a prominent reverse remodelling,

whereas Case 2 (lower panels) shows a patient with SLT and a reduced degree of reverse remodelling (see cross-sections). Image by the author.

3.4. Echocardiography Assessment Prior to the TAVI procedure and During Follow-up

We performed TTE for all 117 patients using an EPIQ 7C system (Philips Medical System, Andover, MA, USA), equipped with X5-1 matrix transducer. The 2D grey-scale images were recorded over three heart cycles and analysed using QLab software (version 10.0 Philips Medical System, Andover, MA, USA) by one of four experienced echocardiographers, blinded to the CT data. Transaortic peak and mean pressure gradients were calculated using the simplified Bernoulli equation (Table 1). The change in mean pressure gradient was determined by calculating the difference between the pre-procedural pressure gradient values and those obtained during the follow-up period. Laboratory, imaging, and clinical data were evaluated at follow-up study visits by a cardiologist at the same day of CT and echocardiographic imaging (14).

3.5. Endpoint definition for adverse events in patients evaluated for LV reverse remodelling

We defined hospitalization for heart failure as any hospitalization event that lasted for >24 h during the follow-up period, at which patient demonstrated at least two heart failure-related symptoms (i.e. oedema and dyspnoe) and required intravenous diuretic therapy (76).

To ensure the accuracy and integrity of mortality data, official death records from the National Health Insurance Fund were collected and carefully verified. This meticulous process aimed to prevent any loss of patient information during the follow-up period.

Mean follow-up time was 2.6 years for this patient cohort. Composite endpoint was defined as heart failure hospitalization or all-cause mortality during follow-up. Survival time was calculated from the date of TAVI to the date of confirmed death, hospitalization or last contact with the patient. We compared clinical outcomes in patients with more and less than 20% reduction in LV mass (the definition of reverse remodelling) (14).

3.6. TAVI procedure and periprocedural complications

In our study assessing the periprocedeural risk factors and complications in 113 patients prosthetic valves were implanted with the standard technique, using local anesthesia with conscious sedation during the procedure. Transfemoral route was the preferred access, transsubclavian or transcarotid routes were considered as an alternative route. Embolic protection devices were not used in this cohort. Adverse events were defined according to the Valve Academic Research Consortium-3 definitions (VARC-3) (77, 78). Procedural factors such as balloon pre- and postdilatations, the number of attempts to position and events of valve dislocation were evaluated and collected in a dedicated database (Table 2) (79).

3.7. Discharge- and follow-up MRI

In our study evaluating periprocedural complications in 113 patients, we performed discharge brain MRI in the first week (4 days after TAVI on average) to detect cerebral ischemic lesions. Patients were excluded, if there was a contraindication to MRI, or they had poor image quality. After applying the above mentioned exclusion criteria 113 patients were analyzed. The MRI examinations were performed on a 1.5T MR scanner (Achieva, Philips Medical Systems) using an 8-channel head coil after TAVI (referred to as discharge MRI). Fluid-Attenuated Inversion Recovery (FLAIR), T2-weighted, T2*-gradient echo, high resolution 3D T1-weighted gradient echo sequences were obtained with diffusion MRI. MRI was repeated at 6 months (6M) in order to assess the gliotic transformation of procedural ischemic lesions. Follow-up MRI examination was performed with the same protocol. Diffusion MRI acquisitions were performed using a single shot spin echo, echo-planar imaging sequence in 32 diffusion encoding directions with b=800 s/mm2 and one b=0 measurement. Whole brain coverage was obtained with 2 mm-thick contiguous axial slices. From the diffusion MRI dataset averaged diffusion-weighted images commonly referred to as 'trace' and mean diffusivity and ADC maps were automatically derived and used to calculate the ischemic lesion volume (ILV). New ischemic lesions were detected at discharge diffusion-weighted imaging (DWI), and they were considered completely resolved if neither DWI nor FLAIR positive lesions were detected in the same location at follow-up; gliotic transformation was considered if there

was FLAIR hyperintensity in the same location of the discharge DWI positive lesion (51, 79).

3.8. Assessment of DTI metrics and white matter region of interests

Diffusion MRI data was processed in the Matlab-based ExploreDTI toolbox (80). To correct distortions originating from patient motion, the diffusion weighted images ($b = 800$) were registered to the first $b = 0$ measurement volume. Motion artifacts and distortions caused by variations in magnetic susceptibility, as well as those associated with the echo-planar imaging readout, were simultaneously corrected in a single interpolation step. This correction was achieved by aligning each subject's 3D T1-weighted images as the registration target (81). Robust tensor fitting with outlier rejection was performed (82) and the average MD, AD, RD and FA values in ROI covering major WM tracts were calculated on the corrected diffusion MRI data. We included 78 subjects into the DTI substudy with complete and adequate discharge and 6M follow-up MRI datasets. The Johns Hopkins University WM tractography atlas was used for WM segmentation [44]. The atlas labels were transformed to each subject's individual image space, for which ExploreDTI utilises the Elastix software [45]. Seven WM ROIs were analysed: 3 callosal segments (genu, body, splenium of the corpus callosum) and 2 bilateral parts of the cingulum (right/left cingulate gyrus and right/left parahippocampal cingulum). These ROIs were subsequently corrected manually to avoid contamination from the grey matter or cerebrospinal fluid using the drawing functions of MRIcron (www.nitrc.org) by an experienced neuroradiologist (Figure 3) (51).
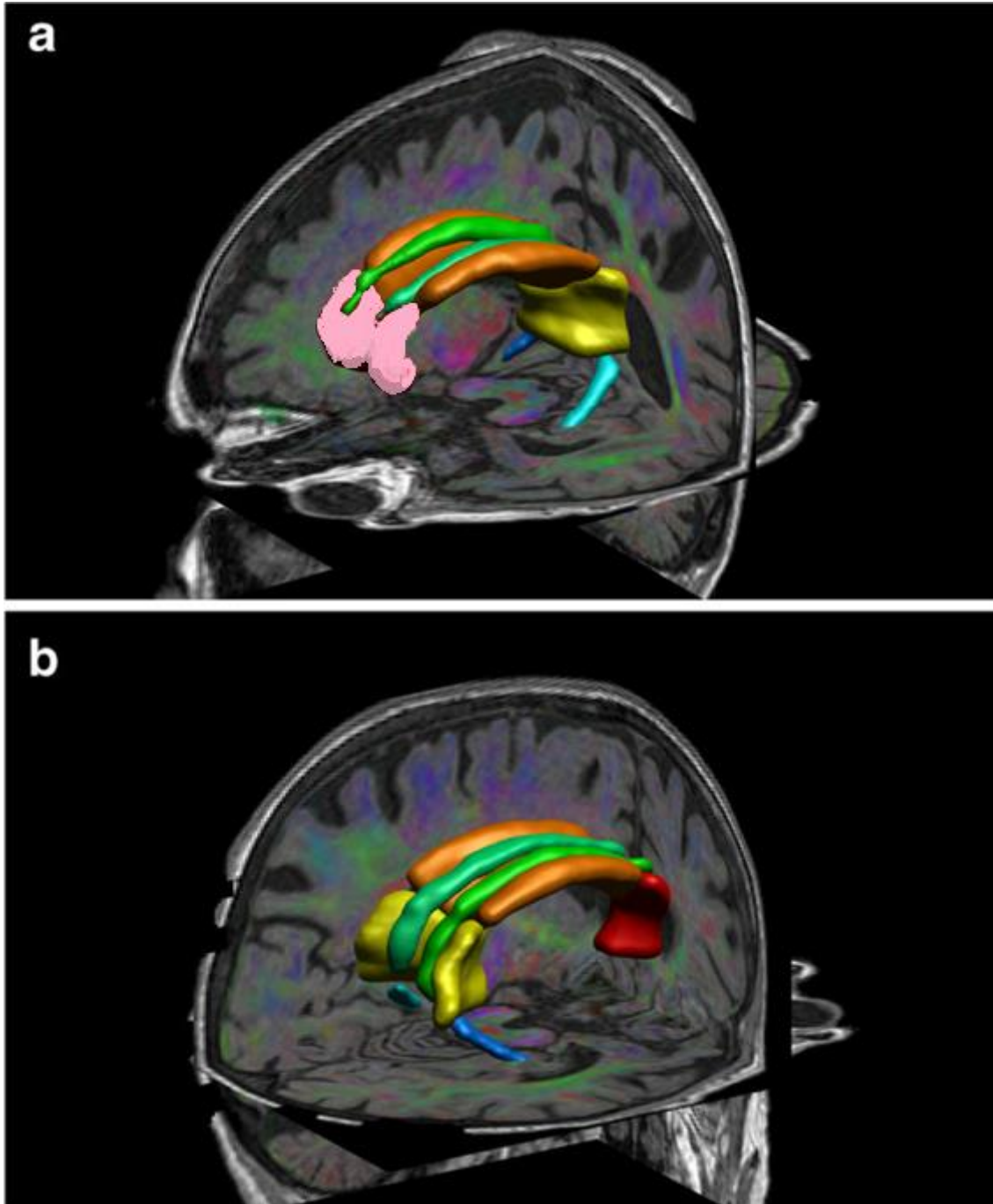
Figure 3. A 3D left anterior–posterior view; b 3D right posterior-anterior view of one study subject's regions of interest projected over the fused colour coded fractional anisotropy and T1 weighted images. Purple = genu of corpus callosum, orange = body of corpus callosum, yellow = splenium of corpus callosum, emerald green = right cingulate gyrus, jade green = left cingulate gyrus, dark blue = right parahippocampal cingulum, light blue = left parahippocampal cingulum. Image by the author.

3.9. Ischemic lesion volume measurement

The localisation, number and size in three perpendicular diameters of all lesions with restricted diffusion were recorded using a PACS workstation (Impax 6.5.2.657, Agfa HealthCare). ILV was calculated as the sum of lesion volumes using the formula of a x b x c x 0.52 (a, b and c are the three lesion diameters) (83). The ILV measurements were performed in a random order and the investigator was blinded to the scan date and patient data (51,79).

In the DTI substudy based on ILV three groups were created as follows:

- Group I: patients with ILV < 100 mm3 (31 subjects).

- Group II: 100 mm3 < ILV < 300 mm3 (25 subjects).

- Group III: 300 mm3 < ILV (22 subjects)

3.10. Neurocognitive assessment

Patients underwent a serial evaluation of the cognitive status pre-TAVI, post-TAVI before hospital discharge, 6M, and 1Y following TAVI. We used the Hungarian version of the Addenbrooke's Cognitive Assessment (ACE) test (84), which encorporated the Mini Mental State Examination (MMSE), and the evaluation was performed by one of two trained investigators blinded to CTA and MRI data (51,79).

Among all enrolled patients 113 participants completed the pre-TAVI, 83 subjects the post-TAVI, 93 subjects the 6M, finally 79 patients the 1Y cognitive tests. Patients with periprocedural stroke (6/113, 5.3%) were excluded from the further neurocognitive assessment. Inclusion criterion of the cognitive study was the accomplishment of the pre-TAVI baseline and at least one of the three further neurocognitive tests (divided into "DTI cognitive" and "non-DTI cognitive" cohorts) (51,79).

3.11. Statistical analysis

Continuous variables are presented as mean and standard deviation, whereas categorical variables are presented as frequency with percentages. Categorical variables were compared using the chi-squared test. Continuous clinical and imaging variables between baseline, discharge and follow-up were compared using Wilcoxon signed-rank test.

To detect the association between LV reverse remodelling and clinical parameters, echocardiographic parameters, cardiovascular risk factors, and SLT univariate and multivariate logistic regression analyses were performed according to our first objective. To assess the prognostic value of LV reverse remodelling Cox proportional hazard regression models were derived. Kaplan–Meier curves were generated for the composite endpoint of hospitalization for heart failure and all-cause mortality (14).

Regarding our second aim, Kruskall-Wallis test was used to analyse the association between ILV and the number of positioning of the valve during TAVI. Because of non-normal distribution of ILV, data were log-transformed. Univariate linear regression analysis was performed to detect the association between patient and procedural related risk factors and log-transformed ILV. Multivariate linear regression models were performed using the backward method. We also aimed to identify predictors of periprocedural stroke using uni- and multivariate logistic regression. Repeated-measures analysis of variance was performed to evaluate changes in neurocognition over time; pairwise differences were assessed using Duncan's multiple comparison test (79).

To evaluate the differences between the averages of discharge TAVI and 6M DTI scalar metrics (FA, AD, MD, AD) student's two tailed, paired sample t-test was used. Bonferroni correction for the 7 ROI comparisons was employed; p-values < 0.0071 were considered significant. The effects of sex, ILV, and age on the DTI metric changes from discharge to 6M MRI were assessed using repeated measures analysis of variance (ANOVA) ($p < 0.05$) with post hoc tests between each pair of ILV groups in Matlab (MATLAB 8.3, The MathWorks Inc, Natick, MA, 2000). Regarding the three pairwise comparisons in the post hoc analysis, we applied Bonferroni correction and $p < 0.0167$ was considered significant. The increase or decrease of each DTI metric was appreciated with the help of box plots. Spearman correlation test was performed to analyse the association of DTI metrics in each ROI and the cognitive results using Matlab ($p < 0.0071$). We analysed the ACE and MMSE scores of the DTI study participants (DTI cognitive cohort) and those who underwent only cognitive testing without DTI (labelled as non-DTI cognitive cohort) with the Kruskal–Wallis test. We also compared the trends of all cognitive domains between the DTI and non-DTI groups using box plots (51).

In other statistical test p value <0.05 was considered statistically significant for all studies. All calculations were performed using SPSS software (SPSS version 23; IBM Corp.).

4. Results

4.1. Assessment of LV reverse remodelling after TAVI

In total 144 patients were included in this study. 7 patients were excluded because of inadequate image quality for the assessment of LVM, or the presence of HALT. Due to the presence of a contraindication, in 20 cases follow-up CT could not be performed, therefore, these patients were excluded. In effect a total, 234 CTAs of 117 patients (mean age 79.0 ± 7.5 years, 53.8% female, mean BSA and mean BMI 26.9 ± 4.7 kg/m2) were included in the final analysis. 24.8% of the patients had prior myocardial infarction, 98.3% had hypertension and 78.6% had hyperlipidemia. Oral anticoagulant medication was administered in 30.8% of all cases. HALT was reported in 30/117 (25.6%) cases. Patient characteristics and imaging data are summarized in Table 1. All patients were successfully implanted with CoreValve (76.1%), Evolut R (16.2%), Portico (6.0%) or Lotus (1.7%) self-expandable valves (14).

Table 1. Patient characteristics

Parameters	n=117
Male, n (%)	54 (46.2)
Age, years	79.0 ± 7.5
Body mass index, kg/m2	26.9 ± 4.7
Body surface area, m2	1.8 ± 0.2
Cardiovascular risk factors	
Hypertension, n (%)	115 (98.3)
Diabetes mellitus, n (%)	34 (29.1)
Hyperlipidaemia, n (%)	92 (78.6)
Smoking in history, n (%)	40 (34.2)
Prior myocardial infarction, n (%)	29 (24.8)

Echocardiographic parameters

Mean aortic transvalvular gradient (pre-TAVI) mmHg	52.2 ± 14.6
Mean aortic transvalvular gradient (Follow-up) mmHg	8.8 ± 4.6
Peak aortic transvalvular gradient (pre-TAVI) mmHg	85.9 ± 23.1
Peak aortic transvalvular gradient (Follow-up) mmHg	16.7 ± 8.3
Change in mean aortic transvalvular gradient	43.4 ± 15.2
Change in peak aortic transvalvular gradient	69.1 ± 24.4

Medication

Statin therapy, n (%)	84 (71.8)
ACE-I/ARB therapy, n (%)	94 (80.3)
Beta-blocker therapy, n (%)	90 (76.9)
Oral anticoagulant therapy, n (%)	36 (30.8)
Dual antiplatelet therapy, n (%)	36 (30.8)

ACE-I: Angiotensin-converting-enzyme inhibitor; ARB: Angiotensin II receptor blockers; BMI: Body mass index; BSA: Body surface area

Continuous variables are presented as mean ± SD, categorical parameters are presented as frequencies and percentages.

LVM and LVMi decreased substantially following TAVI 180.5 ± 53.0 vs. 137.1 ± 44.8 g ($p<0.001$) and 99.7 ± 25.4 vs. 75.4 ± 19.9 g/m2 ($p<0.001$) for pre- and post TAVI respectively) (Figure 4).
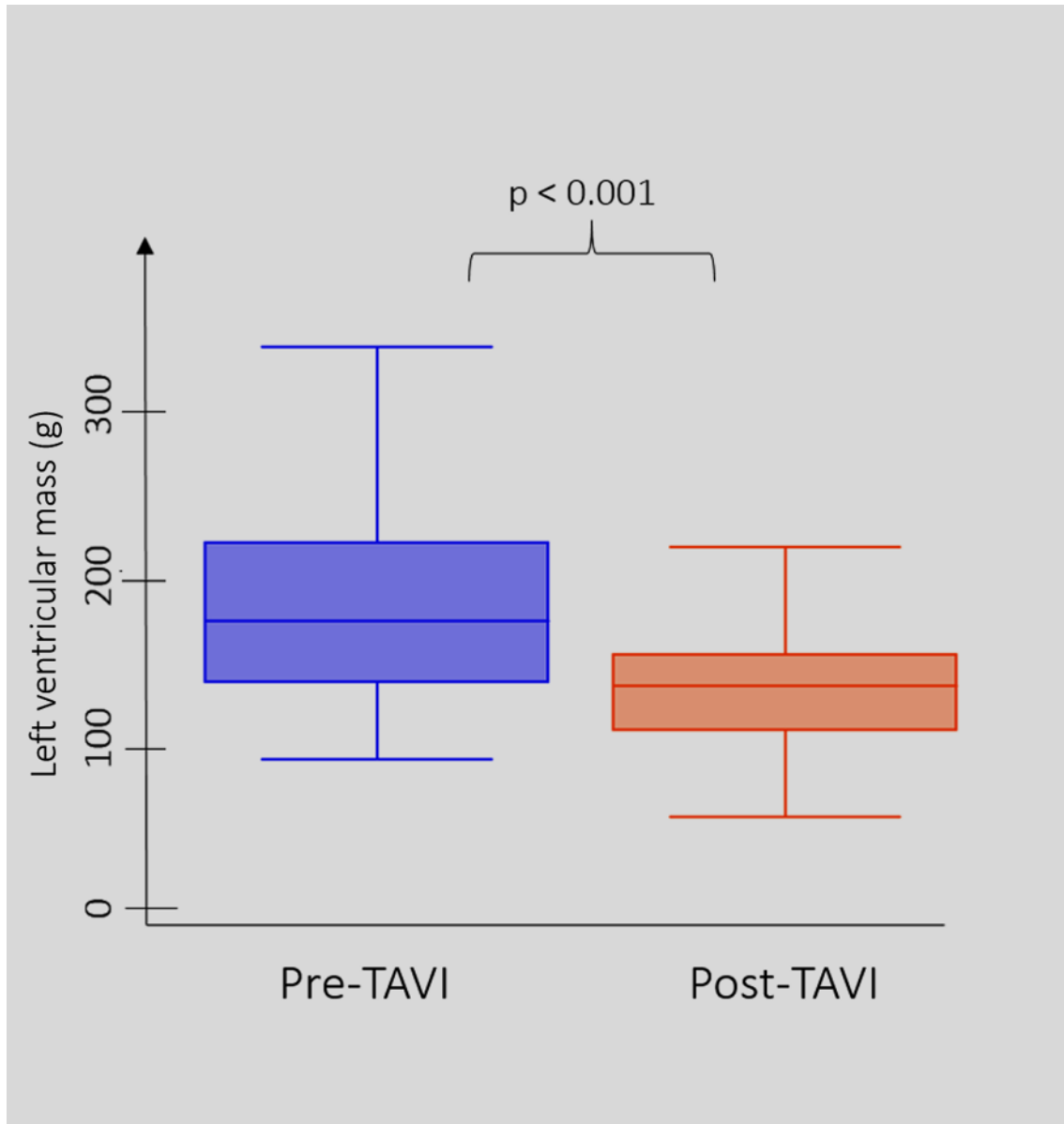
Figure 4. Boxplots demonstrating the impact of TAVI on LVM

We detected an average 43.4 grams reduction in LVM which corresponds to a 22.8 % change after TAVI. In 73/117 patients (62.4%) we found more than 20 % reduction in myocardial mass. We also found that patients with lesser LV reverse remodelling had significantly higher prevalence of SLT and prior myocardial infarction (all $p < 0.05$, Table 2). A larger reduction in transaortic mean and peak pressure gradient values at follow-up were detected among patients with reverse remodelling as compared with those without (both $p < 0.05$, Table 2). Image by the author.

Table 2. Reverse remodelling after TAVI.

	Patients with less than 20% reverse remodelling (N=44)	Patients with more than 20% reverse remodelling (N= 73)	P value
Male, n(%)	25 (56.8)	44 (60.3)	0.072
Age, years	78.4 ± 9.4	79.4 ± 6.0	0.504
Body mass index, kg/m^2	26.4 ± 4.3	27.3 ± 5.0	0.302
Hypertension, n(%)	44 (100)	71 (97.3)	0.268
Diabetes mellitus, n(%)	14 (31.8)	20 (27.4)	0.610
Hyperlipidaemia, n(%)	35 (79.5)	57 (78.1)	0.852
Prior myocardial infarction, n(%)	19 (43.2)	10 (14.0)	**<0.001**
Medication			
Statin therapy, n(%)	32 (72.7)	52 (71.2)	0.862
ACE-I/ARB therapy, n(%)	38 (86.4)	56 (76.7)	0.203
Beta-blocker therapy, n(%)	37 (84.1)	53 (72.6)	0.153
Oral anticoagulant therapy, n(%)	16 (36.4)	20 (27.4)	0.309
SLT	17 (38.6)	13 (17.8)	**0.012**
Change in mean aortic transvalvular pressure gradient (Hgmm)	34.6 ± 11.6	48.9 ± 14.6	**<0.001**

Change in peak aortic transvalvular pressure gradient (Hgmm)	54.8 ± 19.1	70.1 ± 23.1	**<0.001**

ACE-I: Angiotensin-converting-enzyme inhibitor, ARB: Angiotensin II receptor blockers, SLT: Subclinical leaflet thrombosis

Continuous variables are presented as mean ± SD, categorical parameters are presented as frequencies and percentages.

4.1.1. Predictors of LV reverse remodelling

We evaluated clinical and imaging parameters for association with LV reverse remodelling (Table 3-uni- and multivariate analysis). We did not find any association between age, gender, valve type, anticoagulant therapy or cardiovascular risk factors or paravalvular leak and between reverse remodelling (all p>0.05). In univariate analysis, we found that previous myocardial infarction (p = 0.002), the change in mean aortic transvalvular pressure gradient (p = 0.002) and the presence of SLT (P = 0.025) showed a significant association with LV reverse remodelling following TAVI. We found that SLT was inversely and independently associated with LV remodelling over age, gender, prior myocardial infarction change in mean pressure gradient and traditional risk factors (hypertension, dyslipidaemia, body mass index, and diabetes mellitus) in multivariate logistic regression analysis; OR 0.27, P = 0.022 (Table 3). The number of leaflets affected by SLT did not show an association with reverse remodelling (P = 0.391).

Table 3. Predictors of LV reverse remodelling following TAVI.

Parameters	Univariate model		Multivariate model	
	OR	P value	OR	P value
ACE-I/ARB therapy	0.57	0.311		
Myocardial infarction in history	0.28	**0.002**	0.22	**0.006**
SLT	0.35	**0.025**	0.27	**0.022**
Atrial fibrillation	0.74	0.497		
Oral anticoagulant therapy	0.79	0.599		
Change in mean aortic transvalvular pressure gradient (10 Hgmm change)	1.52	**0.002**	1.51	**0.004**

Parameters with significant association with LV reverse remodelling on univariate regression were entered into a multivariate model and also the model was also corrected for age, gender and following risk factors: hypertension, BMI, diabetes mellitus and hyperlipidaemia.

ACE-I: Angiotensin-converting-enzyme inhibitor; ARB: Angiotensin II receptor blockers; OR: Odds ratio; SLT: Subclinical leaflet thrombosis

4.1.2. Prognostic relevance of LV reverse remodelling

Over an average follow-up period of 2.6 years, a total of 13 adverse events were recorded, including 9 deaths and 4 hospitalizations due to heart failure. Patients who showed a reduction in left ventricular (LV) mass of more than 20% following TAVI demonstrated better event-free survival compared to those with a lower degree of reverse remodelling (Figure 5). The reduction in LV mass by more than 20% remained a significant independent predictor of event-free survival even after considering other relevant factors in the multi-variate analysis (HR: 0.27; p=0.0033) (see Table 4).
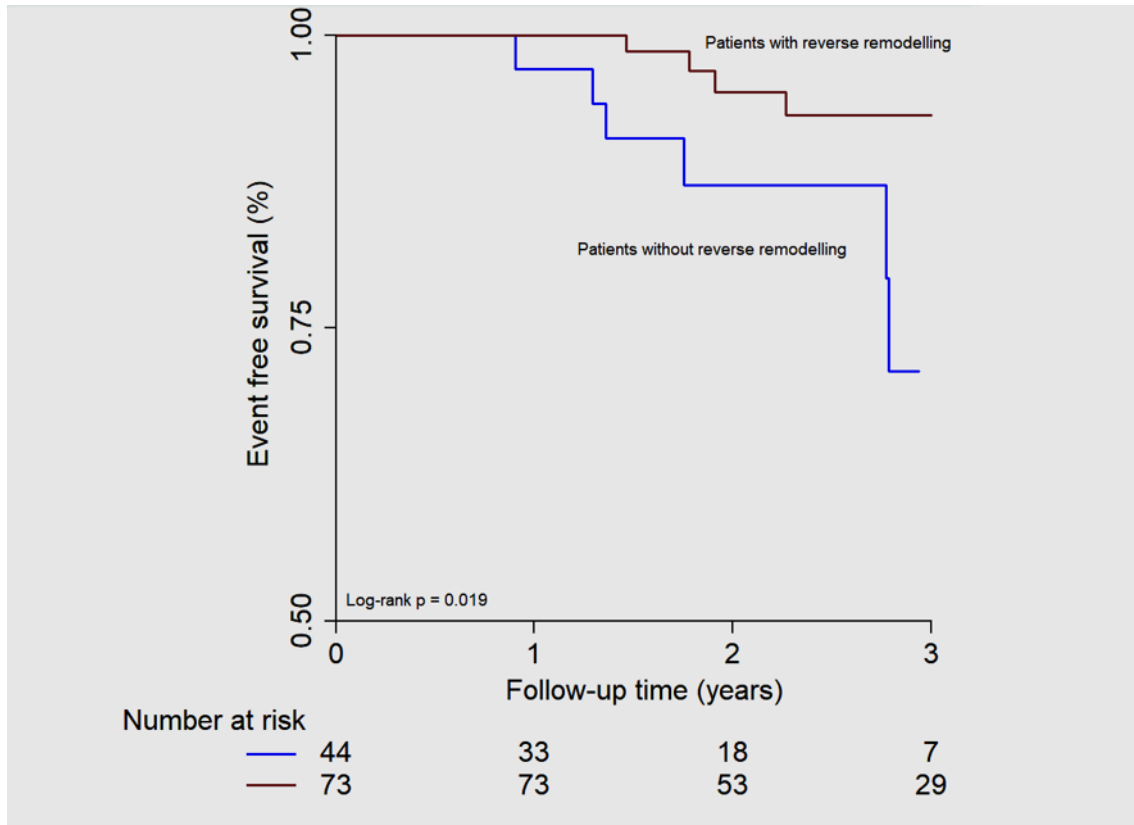
Figure 5. Kaplan Meier curve for mortality and repeat hospitalization following TAVI. Patients with reverse remodelling (defined as >20% decrease in myocardial mass -red line) had improved clinical outcome as compared with patients without reverse remodelling (blue line; log-rank P= 0.019). During a mean follow-up time of 2.6 years, 13 adverse events occurred. Image by the author.

Table 4. Cox regression models to define independent predictors of events

	Univariate model		Multivariate model	
	HR	P value	HR	P value
Age	1.07	0.149		
Body mass index	1.01	0.925		
Diabetes mellitus	4.13	**0.016**	3.57	**0.031**
Hypertension	20.63	0.763		
ACE-I/ARB therapy	0.68	0.591		
Myocardial infarction in history	1.54	0.481		
Reverse remodelling >20%	0.23	**0.019**	0.27	**0.033**
SLT	0.87	0.829		
Atrial fibrillation	1.36	0.604		
Oral anticoagulant therapy	1.56	0.445		
Change in mean aortic transvalvular pressure gradient	0.964	0.102		

ACE-I: Angiotensin-converting-enzyme inhibitor; ARB: Angiotensin II receptor blockers; OR: Odds ratio; SLT: Subclinical leaflet thrombosis

4.2. Predictors and neurological consequences of periprocedural cerebrovascular events following TAVI

Among all patients, 113 patients were included in the analysis evaluating the periprocedural findings and complications (mean age 79.2 ± 6.7 years, 65.8% male, and mean BMI 27.3 ± 4.7 kg/m2). Overall, 23.9% (27/113) of the patients had prior myocardial infarction, 90.3% (102/113) had hypertension and 65.5% (74/113) had hyperlipidaemia. Oral anticoagulant medication was administered in 29.2% (33/113), while 74.3% (84/113) of the patients received antiplatelet therapy. Patient characteristics are summarized in Table 5.

Table 5. Demographic parameters and cardiovascular risk factors

Patient data (N=113)	
Age (years)	79.2 ± 6.7
Female sex, n (%)	50 (44.2)
BMI (kg/m^2)	27.3 ± 4.7
Diabetes, n (%)	54 (47.8)
Hypertension, n (%)	102 (90.3)
Hyperlipidemia, n (%)	74 (65.5)
Previous AMI, n (%)	27 (23.9)
PAD, n (%)	57 (50.4)
Atrial fibrillation, n (%)	38 (33.6)
Previous TIA/stroke, n (%)	15 (13.3)
Chronic kidney disease	64 (56.6)
Antiplatelets, n (%)	84 (74.3)
Anticoagulants, n (%)	33 (29.2)

BMI: Body mass index; AMI: Acute myocardial infarction; PAD: Peripheral artery disease; TIA, Transient ischemic attack.

Continuous variables are expressed as mean ± standard deviation (SD) and categorical variables are expressed as numbers and percentages.

4.2.1. Procedural characteristics

Procedural characteristics and procedural complications are summarized in Table 6. Prosthetic valves were implanted successfully in all patients (Medtronic CoreValve 8.0%, Medtronic CoreValve Evolut R 66.3%, Portico 25.7%). The mean AVCS was 3332 ± 1944, 13.3% patients had a bicuspid aortic valve (BAV). Transfemoral approach was used in 105 cases (92.9%), transsubclavian acces in 6 patients (5.3%), while transcarotid route in 2 cases (1.8%). Balloon predilatation was performed in 15 patients (15.3%), while most of the valves (78.8%) were postdilated. According to the operators' visual judgement, predilatations were performed in case of heavily calcified native aortic valve, however no significant difference in AVCS could be observed in patients with predilatation compared to those without predilatation (median AVCS: 2774 [IQR:1885-4271] vs. median AVCS: 3612 [IQR:1847.4-6366]; p=0.44). The mean number of positional attempts was 1.7 ± 0.9. In 60 (53.1%) cases, the implantation was successful at the first positional attempt, in 39 (34.5%) cases at the second, and in 14 patients (12.4%) at the third or fourth time. According to the VARC-3 criteria 9 patients had major and 17 patients had minor vascular and access-related complications.

Table 6. Procedural characteristics

Patient data (N=113)	
Aortic valve calcium score	3322 ± 1945
Bicuspid aortic valve, n (%)	15 (13.3)
Access route (TF vs. TS/TC), n (%)	105 (92.9) vs. 6 (5.3) vs. 2 (1.8)
Predilatation, n (%)	15 (13.3)
CoreValve vs. EvolutR vs. Portico, n (%)	9 (8.0) vs. 75 (66.3) vs. 29 (25.7)
Number of attempts to position	1.7 ± 0.9
Malposition/Migration, n (%)	5 (4.4)
Postdilatation, n (%)	89 (78.8)
New-onset atrial fibrillation n (%)	8 (7.1)
Vascular and access-related complications, n (%)	26 (23.0)
Minor (according to VARC-3 criteria)	17 (15.0)
Major (according to VARC-3 criteria)	9 (8.0)

VARC-3: Valve Academic Research Consortium, TF: Transfemoral, TS: Transsubclavian, TC: Transcarotid

Continuous variables are expressed as mean ± standard deviation (SD) and categorical variables are expressed as numbers and percentages

4.2.2. Cerebral embolization after TAVI in the study evaluating periprocedural characteristics

We detected new cerebral ischemic lesions on discharge brain MRI in 104 patients (92.0%) (Figure 6), among them 6 (5.3%) patients had periprocedural stroke. The median number of lesions per patient was 6 (IQR: 2-10), and the median ILV was 257.3 µl (IQR: 97.1-718.8 µl). 944 new ischemic brain lesions were found on brain MRI, most of the lesions were supratentorial (781/944, 81.9%), and the majority were located in the cortical subcortical area (796/944, 84.3%). The left and right cerebral and cerebellar hemispheres were equally affected (Table 7). On the follow-up 6M MRI 46/113 (40.7%) patients had gliotic transformation on FLAIR images. Most of the lesions were under 5 mm (558,
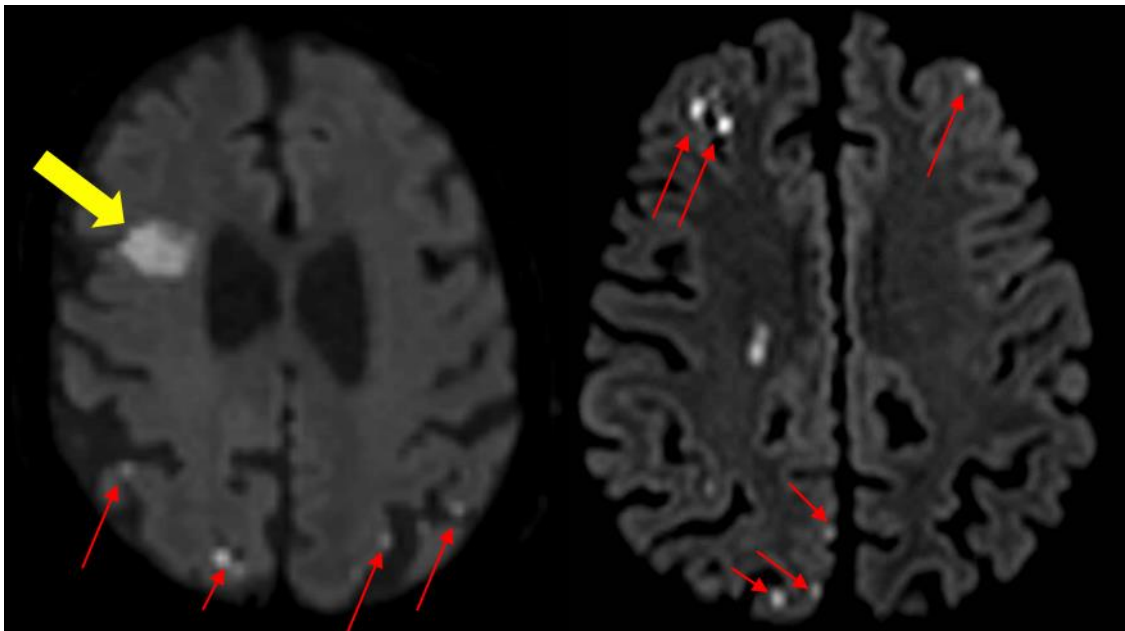
59.1%).

Figure 6. New ischemic lesion after TAVI. Yellow arrow demonstrates a larger lesion with restricted diffusion in the right frontal lobe (left). Red arrows show smaller cortical-subcortical lesions with restricted diffusion in the left and right parietal and frontal lobes. Image by the author.

Table 7. Results of discharge assessment with MRI

Patient data (N=113)	
Patients with new cerebral ischemic lesions, n (%)	104 (92.0)
Patients with periprocedural stroke, n (%)	6 (5.3)
Number of lesions per patient	6 [2-10]
Ischemic load per patient (µl)	257.3 [97.1-718.8]
Number of lesions: left vs. right, n (%)	500 (52.97) vs. 444 (47.03)
Volume of lesions: left vs. right (µl)	123.3 [29.7-357.9] vs. 89.1 [14.6-226.1]
No. of lesions: supra- vs. infratentorial, n (%)	781 (82.7) vs. 163 (17.3)
Volume of lesions: supra- vs. infratentorial (µl)	58.3 [14.58-215.6] vs. 0.0 [0.0-53.1]
Cortical-subcortical lesions, n (%)	796 (83.4)
Deep lesions, n (%)	158 (16.6)
Lesions <5 mm, n (%)	558 (59.1)
Lesions 5-10 mm, n (%)	332 (35.2)
Lesions > 10 mm, n (%)	54 (5.7)

Continuous variables are expressed as median and interquartile ranges [IQR] and categorical variables are expressed as numbers and percentages.

4.2.3. Predictors of ischemic lesion volume and stroke after TAVI

In order to identify potential predictors of ILV and stroke, the association of various clinical and imaging parameters were investigated. Age, cardiovascular risk factors, aortic calcification, access route, valve type and size, and postdilatation did not show any association with ILV (all statistically non-significant, $p>0.05$, Table 8). We found that sex, AVCS, number of valve positioning attempts, and predilatation showed association with log-transformed ILV in univariate analysis. AVCS was not an independent predictor of log-transformed ILV after adjustments. Regarding ILV, it seems that the manipulations during TAVI are more relevant than the aortic valve calcification: positioning the device three or more times resulted in a significant increase in ILV (Figure 7).
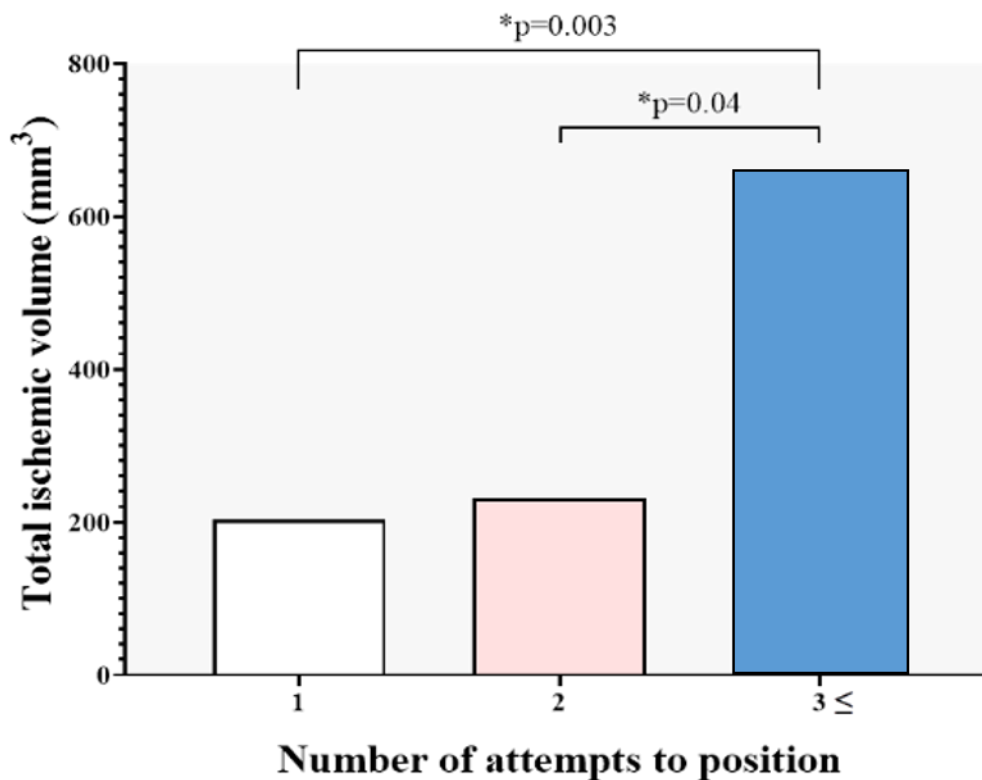
Figure 7. Total ischemic volume on MRI and the number of TAVI positioning attempts. The number of procedural manipulations shows a strong correlation with the ischemic lesion volume (ILV), Three or more positioning attempts of the device resulted in significantly increased ILV. Image by the author.

In multivariate linear regression analysis, predilatation (β=1.13, 95% CI:0.32-1.93; p=0.01), and positioning attempts (β=0.28, 95 % CI: 0.06-0.50; p=0.02) were independent predictors of log-transformed ILV after adjusting for covariates using the backward method (Table 8). We found that predilatation (OR:12.04; 95%CI: 1.46-99.07; p=0.02) and alternative access route (OR: 7.84; 95%CI: 1.01-61.07; p=0.049) were independent factors of periprocedural stroke in multivariate logistic regression analysis (Table 9).

Table 8. Multivariate linear regression analysis of the predictors of total ILV.

	Univariate				Multivariate			
	β	95% CI, lower-upper		p	β	95% CI, lower-upper		p
Sex	*0.48*	*0.10*	*0.86*	*0.02*	0.25	-0.15	0.66	0.22
New-onset AF	0.65	-0.11	1.40	0.09				
Previous AF	0.39	-0.02	0.80	0.06	0.33	-0.04	0.71	0.08
Anticoagulant therapy	0.002	-0.008	0.01	0.65				
Previous stroke/TIA	0.14	-0.45	0.74	0.64				
Aortic valve ca score	*0.00*	*0.00*	*0.00*	*0.02*	0.00	0.00	0.00	0.055
Bicuspid aortic valve	-0.22	-1.03	0.59	0.59				
Alternative access route	0.50	-0.26	1.26	0.19	0.68	-0.04	1.40	0.06
Predilatation	*0.93*	*0.08*	*1.79*	*0.03*	*1.13*	*0.32*	*1.93*	*0.01*
Malposition	0.24	-0.71	1.19	0.62				

Postdilatation		-0.17	-0.65	0.31	0.49			
Number of attempts to position	**to**	**0.23**	**0.03**	**0.44**	**0.03**	*0.28*	*0.06*	*0.50*	*0.02*

AF: Atrial fibrillation; CI: Confidence interval; TIA: Transient ischemic attack. Numbers marked in bold are significant predictors of the outcome based on multivariate analysis (p<0.05).

Table 9. Multivariate logistic regression analysis of the predictors of periprocedural stroke.

	Univariate			Multivariate		
	OR	95% CI, lower-upper	p	OR	95% CI, lower-upper	p
Sex	2.65	0.47 -15.11	0.27			
New-onset AF	2.86	0.29-27.92	0.37			
Previous AF	-0.99	0.17-5.64	0.99			
Anticoagulant therapy	-0.04	-0.75-1.23	0.77			
PAD	0.98	0.19-5.08	0.98			
Previous stroke/TIA	1.58	0.17-14.72	0.69			
Aortic valve ca score	1.00	1.00-1.00	0.99			
Bicuspid aortic valve	3.62	0.60-21.74	0.21			
Alternative access route	*8.42*	*1.28-55.53*	*0.03*	*7.84*	*1.01-61.07*	*0.049*
Pre-dilatation	*12.88*	*1.80-92.27*	*0.01*	*12.04*	*1.46-99.07*	*0.02*
Malposition	0.00	0.00-0.00	1.00			
Post-dilatation	0.52	0.09-3.01	0.46			

| Number of attempts to position | 1.49 | 0.81-2.75 | 0.20 |

AF: Atrial fibrillation; CI: Confidence interval; PAD: Peripherial artery disease; TIA: Transient ischemic attack. Numbers marked in bold are significant predictors of the outcome based on multivariate analysis (p<0.05).

4.2.4. Changes in neurocognitive function

In total of 79/113 patients had serial neurocognitive assessment and post-TAVI MRI, these subjects were included in our subanalysis. The overall cognitive performance of the cohort was stable over the 1Y follow-up period (Figure 8), with mean baseline, discharge, 6M and 1Y Addenbrooke's scores of 72.3±13.1, 74.8±14.2, 72.8±16.6 and 73.4±13.4, p=0.32 and MMS score: 25.9±2.8, 26.1±3.5, 25.8±4.1 and 26.3±3.0, p=0.92, respectively (Table 10). We found that neither ILV nor the presence of gliotic transformation of these procedural lesions was associated with neurocognitive change at any time during the follow-up period (at discharge, at 6M, at 1Y, p>0.05 for all).
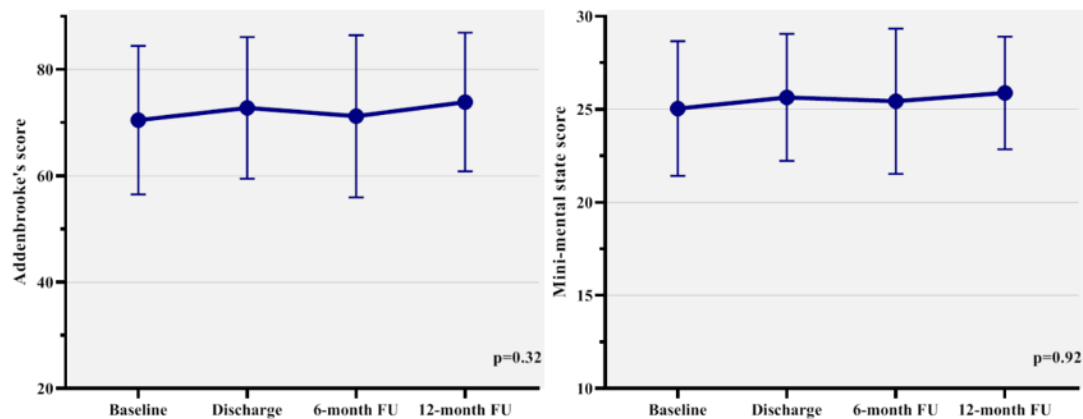
Figure 8. Neurocognitive examination results in the 79 patients based on serial assessments. The overall neurocognitive function was stable during the one-year follow-up (Mean Addenbrooke's and MMS score and SD; p > 0.05 for all.

Table 10. Results of serial neurocognitive assessments.

	Baseline	Discharge	6-month follow-up	1Y follow-up	p
Mini-mental state score	25.9 ± 2.8	26.1 ± 3.5	25.8 ± 4.1	26.3 ± 3.0	0.92
Adenbrook's score	72.3 ± 13.1	74.8 ± 14.2	72.8 ± 16.6	73.4 ± 13.4	0.32

Parameters are shown as mean ± SD

4.3. Assessment of DTI metric changes

4.3.1. Analysis of ischemic volumen**.**

In this substudy 78 subjects were included. The patient characteristics are shown in Table 11. 74 out of 78 study subjects (95%) had recent ischemic lesions with restricted diffusion, 71 of them supratentorial (91%), most of them multiple (57/70, 81%) ranging from 2-20 mm.

We excluded infratentorial ischemic brain lesions (IBLs) from the analysis because we considered that these lesions are not relevant regarding cognitive function. 363 supratentorial lesions were found, more in the left cerebral hemisphere (194 vs 169). The majority of these lesions were small (268/363, 74%, ≤5mm; 109/363, 30%), mostly located at the cortical-subcortical region. The median lesion volume was 38.88 mm3 (range 14 mm^3–17.4 cm^3). Three larger posterior cerebral artery territorial infarcts were detected (two on the left, another one on the right, neither involved our ROIs). With special regard to ischemic injury in our ROIs, if the ROI was affected we excluded from the further analysis. We have to exclude only two ROIs during manual correction, when part of the left parahippocampal cingulum and a small segment of the splenium was affected. At 6 months, 7 out of 78 participants (9%) had new supratentorial IBL(s) with

restricted diffusion: one lesion in 4 subjects, two lesions in 2, finally 7 lesions in 1 subject. The ILV ranged from 14-232 mm^3 (50% of the lesions were dot-like, measuring 3 mm).

Table 11. Age, gender, co-morbidities and medical therapy of the 78 diffusion tensior imaging study subjects

Demographics	n: 78
Male gender n (%)	44 (56)
Mean age ± SD (years)	79 ± 6
Body Mass Index ± SD (kg/m^2)	27.2 ± 4.8
Body Surface Area ± SD (m^2)	1.8 ± 0.2
CHA2DS2-VASc score	5 ± 3
Co-morbidities	
Hypertension n (%)	79 (90)
Diabetes mellitus type2 n (%)	33 (42)
Hyperlipidemia n (%)	53 (70)
Current smoking n (%)	5 (6)
Former smoking n (%)	5 (6)
Atrial fibrillation/flutter n (%)	26 (33)
Previous TIA n (%)	2 (3)
Previous minor stroke n (%)	3 (4)
Coronary artery disease – post myocardial infarction n (%)	17 (22)

Coronary artery disease – no myocardial infarction n (%)	18 (23)
Coronary revascularization – PCI n (%)	26 (33)
Coronary revascularization – CABG n (%)	5 (6)
Non-significant carotid artery stenosis n (%)	40 (51)
Previous carotid artery intervention n (%)	3 (4)
Heart failure NYHA II n (%)	40 (51)
Heart failure NYHA III n (%)	34 (44)
Heart failure NYHA IV n (%)	4 (5)
Liver disease n (%)	2 (3)
Any malignancy n (%)	15 (19)
Chronic obstructive pulmonary disease n (%)	13 (17)
Renal failure (GFR<30) n (%)	3 (4)

Medication

Anticoagulant therapy (vitamin K antagonist) n (%)	13 (17)
Anticoagulant therapy (NOAC) n (%)	10 (13)
Current antiplatelet therapy (single) n (%)	38 (49)
Current antiplatelet therapy (dual) n (%)	17 (22)
Statin therapy n (%)	50 (64)
ACE inhibitor/ARB n (%)	62 (80)
Beta blocker n (%)	66 (85)

ACE = angiotensin converting enzyme inhibitors; ARB = angiotensin II receptor blocker; BMI = body mass index; CABG = coronary artery bypass grafting; CHA2DS2-VASc = Congestive heart failure, Hypertension, Age, Diabetes, Stroke/TIA and VAScular disease score; NOAC = novel oral anticoagulant; NYHA = New York heart association functional classification; PCI = percutaneous coronary intervention; SD = standard deviation

4.3.2. Analysis of DTI scalar metrics changes

In 4 out of the 7 WM ROIs significant reduction of AD was detected (genu and body: p<0.0001; splenium and right parahippocampal cingulum: p=0.0023), coupled with significant decrease of the MD in the body of corpus callosum (p=0.0006) and FA in the splenium (p<0.0001) using the paired sample t-test with Bonferroni-correction. We found significant reduction of RD and MD in the cingulate gyrus bilaterally significant reduction of RD and MD (right cingulate gyrus: MD - p=0.0025, RD - p=0.0053; left cingulate gyrus: MD - p=0.0004, RD - p=0.0010). The other changes were not significant. (Table 12.)

Table 12. One tailed paired T-test results with Bonferroni-correction of diffusion tensor metrics in seven white matter regions of interest

	DTI metric	mean (SD) baseline	mean (SD) 6-month follow-up	p-value	T
body of CC	FA	0.5402 (0.0401)	0.5371 (0.0379)	0.0739	1.4623
	MD	1.2341 (0.0720)	1.2134 (0.0700)	**0.0006**	3.3586
	AD	2.0252 (0.0974)	1.9854 (0.1033)	**<0.0001**	5.4712
	RD	0.8386 (0.0802)	0.8274 (0.0741)	0.0412	1.7604
righ CG	FA	0.4853 (0.0372)	0.4892 (0.0395)	0.8651	-1.1113
	MD	0.8328 (0.0354'	0.8230 (0.0286)	**0.0025**	2.8961
	AD	1.3173 (0.0699)	1.3070 (0.0657)	0.0562	1.6112
	RD	0.5906 (0.0386)	0.5810 (0.0372)	**0.0053**	2.6212
left CG	FA	0.5207 (0.0405)	0.5251 (0.0410)	0.8675	-1.1229
	MD	0.8215 (0.0306)	0.8099 (0.0289)	**0.0004**	3.5074
	AD	1.3482 (0.0669)	1.3360 (0.0721)	0.0405	1.7685
	RD	0.5581 (0.0374)	0.5469 (0.0356)	**0.0010**	3.1907

	FA	0.4306 (0.0441)	0.4284 (0.0430)	0.3009	0.5239
right PHC	MD	0.8560 (0.0835)	0.8356 (0.0339)	0.0133	2.2615
	AD	1.2831 (0.1053)	1.2514 (0.0500)	**0.0023**	2.9265
	RD	0.6424 (0.0828)	0.6277 (0.0458)	0.0501	1.6643
	FA	0.4246 (0.0357)	0.4211 (0.0387)	0.2038	0.8325
left PHC	MD	0.8273 (0.0547)	0.8213 (0.0419)	0.1720	0.9522
	AD	1.2306 (0.0860)	1.2171 (0.0596)	0.0529	1.6369
	RD	0.6256 (0.0505)	0.6233 (0.0475)	0.3639	0.3493
	FA	0.5556 (0.0426)	0.5495 (0.0404)	0.0202	2.0853
genu of CC	MD	1.1252 (0.0710)	1.1095 (0.0682)	0.0121	2.2989
	AD	1.8902 (0.1113)	1.8523 (0.1161)	**<0.0001**	4.1680
	RD	0.7428 (0.0748)	0.7381 (0.0671)	0.2494	0.6795
	FA	0.6404 (0.0373)	0.6305 (0.0338)	**<0.0001**	4.2235
splenium of CC	MD	1.0249 (0.0687)	1.0269 (0.0640)	0.6559	-0.4028
	AD	1.8682 (0.0923)	1.8504 (0.0886)	**0.0023**	2.9221
	RD	0.6032 (0.0729)	0.6152 (0.0662)	0.9855	-2.2261

CC: corpus callosum; CG: cingulate gyrus; PHC: parahippocampal cingulum; AD: axial diffusivity; FA: fractional anisotropy; MD: mean diffusivity; RD: radial diffusivity; SD: standard deviation; Metric dimensions: FA: dimensionless MD, AD, RD: 10^{-4} mm^2/s;

4.3.3. Effect of sex and age on DTI metric changes

The repeated measures ANOVA confirmed significant effect of female sex on AD/MD reduction. We found significantly greater decrease of AD and MD in women in the body of corpus callosum and in the right cingulate gyrus (body: AD - p=0.0065, MD - p=0.0254; right cingulate gyrus: AD - p=0.0001, MD - p=0.0035) with a significantly greater reduction of AD alone in the left cingulate gyrus (p=0.0062). (Figure 9 and

Supplementary Table 1). No significant effect of age was detected in any of the other studied ROIs.
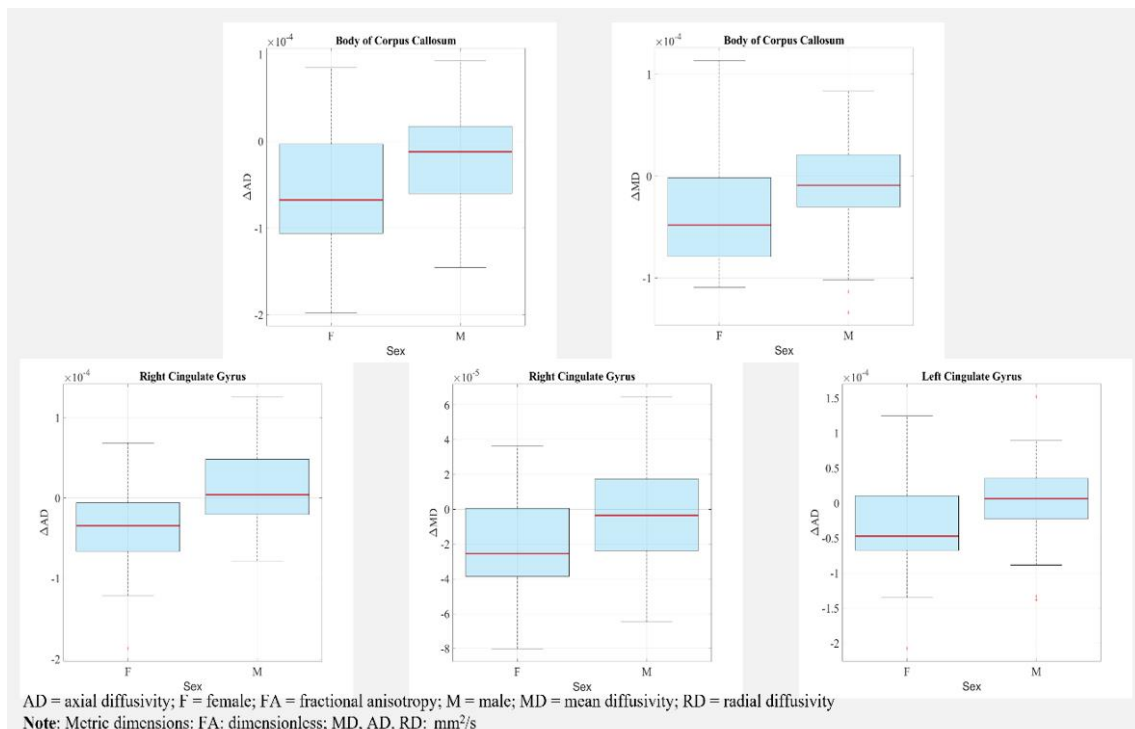
Figure 9. Box plots of significant associations of change in diffusion tensor imaging metrics with sex. Top row: change of axial diffusivity (left) and mean diffusivity (right) from post-TAVI to 6 months in the body of corpus callosum in females versus males. Bottom row: change of axial diffusivity (left) and mean diffusivity (middle) from baseline to 6 months in the right cingulate gyrus; change of axial diffusivity from baseline to 6 months in the left cingulate gyrus (right) in females versus males. (Red line = median; top of box = 25th percentile; bottom of box = 75th percentile; plotted whisker = the most extreme data value that is not an outlier; red cross = outlier) Image by the author.

4.3.4. Effects of ILV on DTI metric changes

The repeated measure ANOVA showed significant effect of ILV on certain DTI metric changes in 3 out of 7 ROIs. Figure 10 and Supplementary Table 1. In the body of the corpus callosum the repeated measures ANOVA detected a significant effect of ILV on the change of AD, MD and RD across the groups (p=0.0045, 0.0050, and 0.0175, respectively). As revealed by the post hoc comparison, the difference was the most pronounced between the ILV group I (decrease of AD and MD) and the ILV group III

(increase of AD and MD); p=0.0183 for AD and p=0.0457 for MD. In group III the RD increased and the FA decreased (as opposed to groups I-II), without reaching the level of significance.

In the left cingulate gyrus significant difference in MD reduction was found between the ILV group II and group III (p=0.0087). The decrease of MD was more marked in the intermediate group relative to the group with the highest ILV.

In the splenium of the corpus callosum the increase of MD differed significantly comparing group II with group III (p=0.0399). The more pronounced increase in MD and a non-significant increase of AD in ILV group III versus the reduction of AD in groups I-II) point towards unfavorable microstructural alteration associated with higher ILV. The other associations were non significant.

AD = axial diffusivity; FA = fractional anisotropy; MD = mean diffusivity; RD = radial diffusivity. NOTE: Metric dimensions: FA: dimensionless
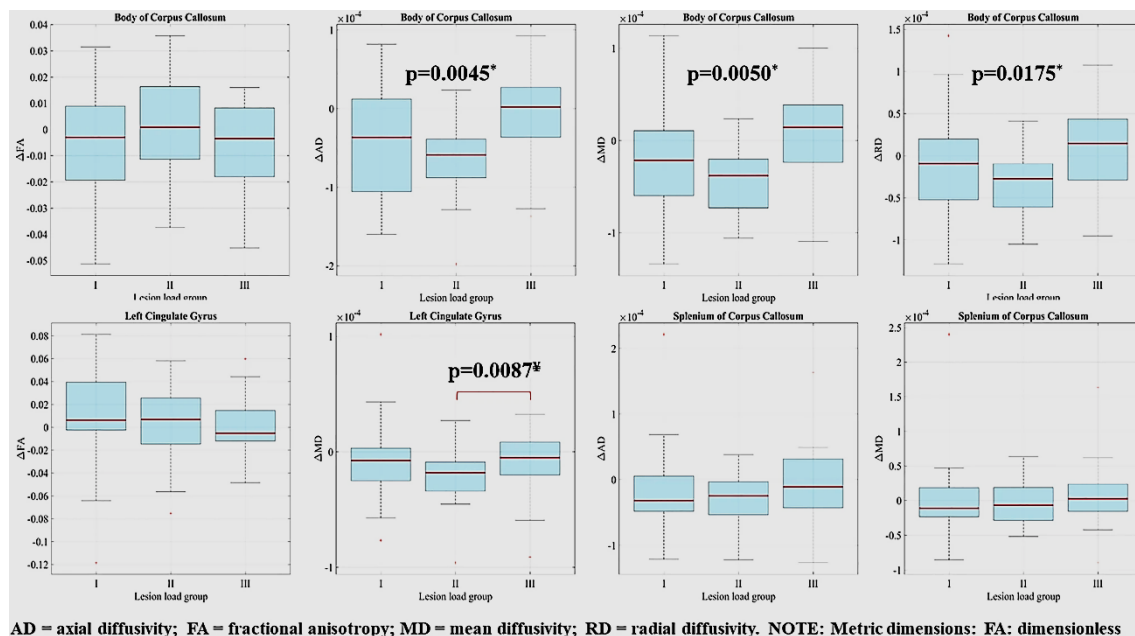
Figure 10. Box plots of association of change in diffusion tensior imaging metrics with ischemic lesion volume (ILV). Top row (from left to right): change of fractional anisotropy, axial diffusivity, mean diffusivity and radial diffusivity from baseline to 6 months in the body of corpus callosum in ILV groups I, II and III. Bottom row (from left to right): change of fractional anisotropy and mean diffusivity from baseline to 6 months in the left cingulate gyrus; change of axial diffusivity and mean diffusivity from baseline to 6 months in the splenium of the corpus callosum in ILV groups I, II and III. (Red line = median; top of box = 25th percentile; bottom of box = 75th percentile; plotted

whisker = the most extreme data value that is not an outlier; red cross = outlier). Image by the author.

* p-values from repeated measures analysis of variance across ILV groups.

¥ p-value from post hoc analysis indicating significant between-group difference

4.3.5. Cognitive trajectory

106 participants completed the pre-TAVI, 83 subjects the post-TAVI, 93 subjects the 6M, finally 79 patients the 1Y cognitive tests. Neurocognitive tests were completed in the DTI group in 51, 42, 57, 49 cases respectively. The Kruskall-Wallis test did not reveal a significant difference in the distribution of ACE and MMSE scores between the DTI and the non-DTI groups, and the corresponding boxplots showed a very similar trend in all cognitive domains, therefore we opted for analysing the cognitive performance of the whole study cohort. Supplement Table 1.

Although there was an improvement in 3 domains and ACE score (Figure 11.), the repeated-measures linear mixed-effect model revealed no significant change in cognitive function over one year. The pre-TAVI cognitive function had a significant effect on later scores at any timepoints ($p < 0.0001$): the lower the ACE score was prior to the intervention, the more pronounced improvement was observed after TAVI. In ILV group III there was a significant decline in retrograde memory ($p = 0.0489$) and visual scores ($p = 0.0151$) compared to ILV groups I+II. Table 13. Apart from the improvement of evocation scores from pre-TAVI to post-TAVI, the Wilcoxon signed-rank test showed no significant change, in particular deterioration, regarding any domains across any different timepoints.
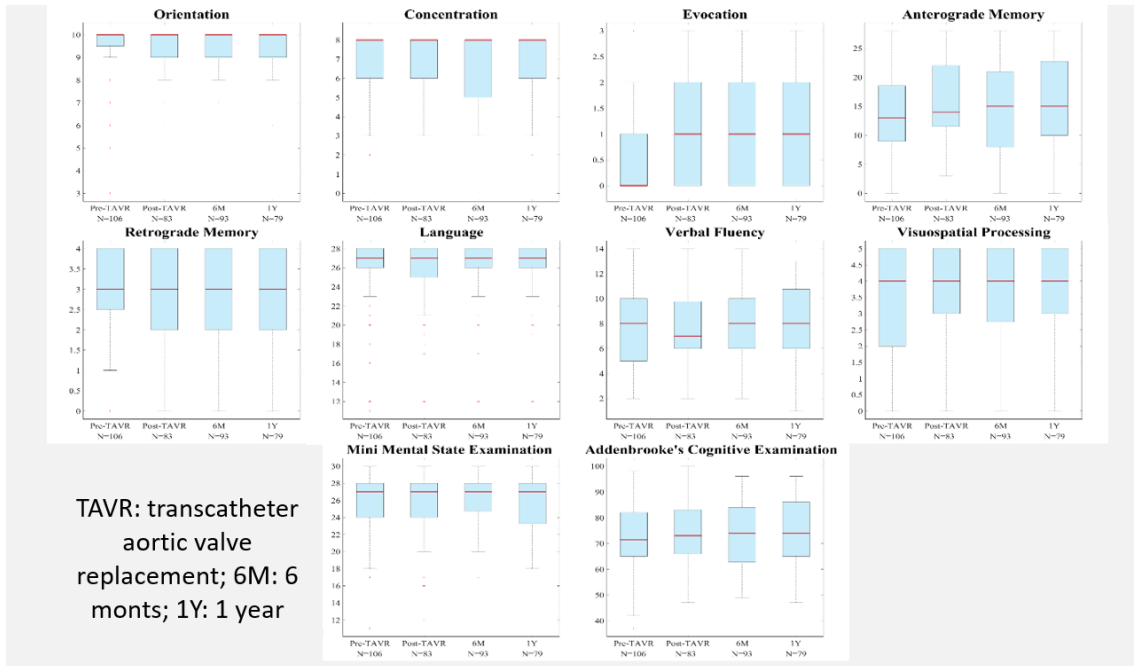
Figure 11. Box plots of cognitive scores pre-TAVR, post-TAVR, at 6 months and 1 year. Red line = median; top of box = 25th percentile; bottom of box = 75th percentile; plotted whisker = the most extreme data value that is not an outlier; red cross = outlier. Image by the author.

Table 13. Trend analysis of cognitive scores over time

Outcome	Variables	Regression coefficient (β)	95% CI	p
ACE score at different timepoints	Intercept	15.3131	4.7209; 25.9053	0.0052
	pre-TAVI score	0.8184	0.6748; 0.9621	**<0.0001**
	Time from TAVI	-0.0358	-0.2508; 0.1792	0.7411
Change of ACE score	Intercept	15.6595	4.9801; 26.3388	0.0046
	pre-TAVI score	-0.1844	-0.3292; -0.0395	**0.0137**
	Time from TAVI	-0.0766	-0.2829; 0.1298	0.4618
Effect of ILV on retrograde memory	Intercept	0.7391	0.0255; 1.4527	0.0425
	pre-TAVI score	0.7499	0.5465; 0.9533	**<0.0001**
	ILV	-0.4175	-0.8328; -0.0021	**0.0489**
	Time from TAVI	-0.0056	-0.0362; 0.0250	0.7189
Effect of ILV on visuospatial processing	Intercept	1.6757	1.0666; 2.2848	<0.0001
	pre-TAVI score	0.5988	0.4433; 0.7542	**<0.0001**
	ILV	-0.5514	-0.9914; -0.1113	**0.0151**
	Time from TAVI	-0.0039	-0.0360; 0.0281	0.8071

ACE: Addenbrooke's cognitive examination; ILV: ischemic lesion volumen; TAVI: transcatheter aortic valve implantation

4.3.6. Correlation of DTI metrics and cognitive output

Low diffusivities showed a trend towards higher cognitive scores in many ROIs but in most cases, it did not reach statistical significance after correction of the p-value for multiple comparisons. However, the negative correlation remained significant in some instances: in the left cingulate gyrus (association of low RD values and high language scores: $p = 0.0012$; low RD and high verbal fluency scores: $p = 0.007$) and in the genu (low AD and high retrograde memory scores: $p = 0.0034$).

5. Discussion

We conducted a prospective study in a large real-world cohort of patients who have underwent TAVI to assess the impact of SLT on LV reverse remodelling and on clinical outcome using CTA, and to evaluate the patient- and procedure-related predictors of new ischemic brain lesions and stroke following TAVI, as well as their occurrence and distribution utilizing diffusion MRI. We also assessed the effect of SCILs on the patients' neurocognitive function. Furthermore, our aim was to detect the microstructural WM changes following TAVI using DTI MRI. The implantation rate of transcatheter bioprosthetic valves is steeply increasing and the indication of TAVI is shifting towards lower risk patients (85, 86), it is therefore crucial to to understand the clinical consequences of HALT, and to accurately identifythe patient- and procedural related risk factors of subsequent ischemic brain lesions and stroke after TAVI, and to better understand their neurological impact and consequences.

5.1. The association of SLT with adverse cardiac remodelling and clinical outcome

CTA imaging has the capability to identify initial alterations in implanted bioprosthetic valves without the need for invasive procedures. At present, there are no established guidelines for the diagnostic evaluation of individuals suspected of subclinical leaflet thrombosis (SLT). However, experts suggest that echocardiographic surveillance should be used to identify patients displaying elevated pressure gradients, thickened valve cusps, or limited cusp movement. Such patients may then be considered for follow-up CT imaging. (87, 88). In our study, the prevalence of SLT was almost 26%, which is in line with the literature (89-91). However, consensus or unified criteria for HALT assessment is needed based on CT images (29, 90, 92). The findings of this study are a valuable addition to the existing literature, as they provide important supplementary evidence regarding the correlation between subclinical leaflet thrombosis and clinical prognosis.

We found that TAVI results in significant LVM reduction. Our findings indicate that the presence of SLT may act as a risk factor, impeding the beneficial changes in left ventricular reverse remodelling following TAVI. Additionally, our findings demonstrated an association between impaired left ventricular reverse remodelling and negative clinical outcomes defined as mortality and heart failure hospitalisation.

Our research provides deeper understanding of how SLT and the process of reverse remodelling interact, emphasizing the importance of structural LV changes in patients treated with TAVI utilizing CTA. Magalhaes et al. examined 333 TAVI patients and sought to evaluate alterations in LV geometry using TTE (93). In their study, reverse remodelling process was not complete even at 1 year following TAVI. Cardiac MRI studies demonstrated that detectable reverse remodelling could be present even within few days after TAVI (94, 95), suggesting that the process of LV recovery can occur more rapidly than previously anticipatedand the most substantial decrease in LVM can be observed in the first few weeks after the transaortic pressure gradient normalizes. Thereafter, there is a trend for a slower and more modest improvement that can last up to a 12-24 months (96, 97). Similarly, studies suggest that the occurrence of HALT varies in time individually (28, 87, 91). HALT can develop within weeks (acute) or months (late) after TAVI, and progress over time without treatment. Makkar et al. found HALT as early as 3-5 days after the TAVI with increasing incidence up to 1 year (98). Subclincal leaflet thrombosis can affect the function of the bioprosthesis which is associated with elevated transvalvular pressure gradients on TEE imaging (87) and thus might impact remodelling processes. These observation are reflected by our results as well.

LV hypertrophy poses an elevated risk for various cardiovascular complications, including sudden cardiac death, congestive heart failure, and adverse cardiovascular events. This increased risk can be attributed to various suggested mechanisms, such as accelerated atherosclerosis, impaired pump function, adverse structural remodelling, and ischemia-related arrhythmias (99, 100). Once the afterload is normalised, a favorable structural alterations can begin in the LV (101, 102). Nonetheless, the extent of these changes varies among individuals, and LV recovery can be influenced by various clinical and imaging factors. Our findings, as well as previous echocardiography and cardiac MRI studies, consistently reveal a substantial decrease in LVM following SAVR (95, 103). In a study by Vizzardi et al. 135 TAVI patients underwent serial TTE imaging, and it was observed that more than 30% of the patients experienced a greater than 30% reduction in LVM. Furthermore, data from the PARTNERregistry indicated a 17% reduction in LVM one year after valve implantation (104). However, the magnitude of changes show individual differences and LV recovery can be influenced by several clinical and imaging parameters. Our results and prior echocardiography or cardiac MRI studies have

consistently demonstrated a significant regression in LVM after AVR (95, 103). In the study of Vizzardi et al. 135 TAVI patients were evaluated using serial TTE imaging, and more than 30% decrease in LVM was detected in 37% of the patients. Also, results from the PARTNER (Placement of Aortic Transcatheter Valves) registry demonstrated a reduction of 17% in LVM 1 year after implantation (104). We found that more than 20% reduction was seen in 66% of the patients corresponding to a 22.8% reduction on average. It remains unclear which patients exhibit complete remodelling of the LV, while in others only partial resolution of LV hypertrophy occurs. Puls et al. found that histological myocardial fibrosis is in correlation with LV remodelling and clinical heart failure, and it is associated with the delay of reverse LV remodelling and clinical benefit following TAVI. They also found that myocardial fibrosis was an independent predictor of cardiovascular mortality after TAVI (105). However, TEE and MRI studies could not evaluate properly HALT as a potentially factor, which may have a significant influence on LV remodelling. We found that HALT and prior myocardial infarction are inversely associated with reverse remodelling and thus can reshape risk prediction in this patient cohort (14).

Identifying the clinical and imaging factors that predict left ventricular (LV) recovery is crucial, as it has been shown that reverse remodelling is linked to improved outcomes following SAVR. Vizzardi et al. found that only the initial LV mass (LVM) value independently predicted subsequent reverse changes (106). Other studies have suggested the severity of aortic regurgitation (107) or myocardial fibrosis as potential risk factors (96, 105). It has been proposed that early adverse remodelling tends to occur in patients without myocardial fibrosis, which may offer long-term benefits. Our results suggest that patients who suffered myocardial infarction (replacement fibrotic changes is already there) – irrespectively of the presence of SLT- have lower reduction in myocardial mass (14).

Comprehensive data regarding the predictive significance of reverse remodelling after TAVI is still limited. Our findings highlight an association between the presence of HALT and limited reverse remodelling and the lower rates of LV reverse remodelling is independently associated with the composite endpoint of death or heart failure hospitalisation. In our study we recorded 13 adverse events during the follow-up with a mean follow-up time of 2.6 years. Significantly higher event rates were observed among

patients with less than 20% reduction in LVM versus those with more prominent LVM changes. However, Kuneman et al. found that improvement in LVEF and LV reverse remodelling was not associated with HALT. They did not find any difference in cardiovascular events in patient with or without HALT (108). This difference between the results could be related to differences in imaging modality to assess LV mass (CTA versus echocardiography) and the timing of assessing LV mass after TAVI (12 months versus 3 months) (14).

Ali et. al have described that lower reduction in LVM was associated with poor long term prognosis in patients after surgical aortic valve replacement using TEE. In the PARTNER randomized trial, the researchers found that a more substantial reduction in left ventricular mass (LVM), as assessed by echocardiography, was linked to decreased hospitalization rates. However, there was no significant variation in all-cause mortality after one year (103). Difference in all-cause mortality as compared with our result might be the result of shorter follow-up time period. Our results are consistent with the previously mentioned findings, demonstrating that more significant regression in left ventricular mass (LVM) following aortic valve replacement could lead to long-term benefits by reducing both all-cause mortality and the frequency of repeat hospitalizations for heart failure. More importantly, HALT and reverse remodelling are proposed as novel imaging targets in the future for post-TAVI patient management.

5.2. Cerebrovascular embolization and events following TAVI, periprocedural data

The main findings of our substudy are the following: 1) 92% of the patients had new cerebral ischemic lesions, however most of them were clinically silent; 2) Balloon predilatation and the number of valve positioning attempts during the procedure were independently associated with a larger log-transformed ILV, whereas predilatation and alternative access route were associated with periprocedural stroke; 3) The ILV was not associated with cognitive decline after TAVI (79).

Despite the extensive research on risk factors for CVE and SCIL during TAVI, the identified predictors differ among studies. This highlights the intricate nature of factors related to both patients and the TAVI procedure itself (31, 33, 35, 36, 39-41, 48, 49, 109-118). While CVEs are relatively uncommon, they pose a major concern in this frail patient

population with multiple comorbidities and are linked to poor outcomes. Nombela-Franco et al. reported that valve dislodgement/embolization and balloon postdilatation were predictors of acute CVE, and new-onset atrial fibrillation was associated with the incidence of subacute CVE (31). Keiko et al. reported that self-expandable valves were independently associated with acute cerebral embolization on MRI after TAVI (112). A meta-analysis described that chronic kidney disease, female sex, new-onset atrial fibrillation and level of operator's experience were associated with CVE post-TAVI (35). Regarding vascular access, Rodés et al. (41) did not observe any significant difference when comparing the transfemoral and transapical approaches. However, Eggebrecht et al. (32) reported an association between stroke risk and the choice of approach, with transapical TAVI showing the lowest risk of stroke. In a meta-analysis conducted by Lu et al. transcarotid access was identified as a predictor of 30-day mortality and was associated with an increased risk of 30-day neurovascular complications (119). A nationwide study conducted in Sweden revealed that diabetes impaired renal function, age, male gender, and a history of stroke were risk factors for stroke after the TAVI procedure (120). Regarding the vascular access, Rodés et al. did not find any difference when comparing transfemoral vs. transapical approaches (41), however Eggebrecht et al. (32) found an association between stroke and the type of approach, with transapical TAVI carrying the lowest risk of stroke. A meta-analysis from Lu et al. found that transcarotid access was a predictor of 30-day mortality, and was associated with an increased risk of 30-day neurovascular complications (119). A nationwide study from Sweden described that impaired renal function, age, diabetes, male sex and history of stroke were risk factors for developing stroke following TAVI (120). Also, a recent meta-analysis showed that next-generation devices were associated with lower risk of TAVI related complications including valve malpositioning, paravalvular regurgirgation and periprocedural stroke as well (34). We found that predilatation and valve positioning maneuvers were significant predictors of larger ILV, while predilatation and the chosen vascular access route were identified as risk factors for periprocedural stroke (79).

SCILs are highly common following TAVI, but their impact on neurocognitive function is still on debate and remains controversial (42, 44, 48, 49, 110). Several brain MRI studies have shown a high incidence (58-91%) of new ischemic lesions after transcatheter aortic valve replacement, regardless of the approach and valve type (40-42, 111). Various,

different predictors for SCIL have been identified: Carlo et al. demonstrated that baseline age-related white matter damage on MRI increased the risk for SCIL, together with the use of non-balloon-expandable prostheses (110). A meta-analysis by Woldendorp found that predilatation, kidney disease, and diabetes were associated with prevalence of SCIL (48).

We found that the number of positioning attempts of the valve resulted a significant increase in log-transformed ILV following TAVI. Interestingly, we did not found correlation between aortic valve calcium score and ILV. Importantly, the vascular access route, the valve type, or the presence of bicuspid aortic valve did not influence the log-transformed ILV either. While the alternative access route did not demonstrate a statistically significant association with indexed left ventricular mass (ILV), there was a noticeable trend. The absence of statistical significance in the ILV and alternative access route relationship could be attributed to the relatively low number of alternative access (7.1%) in our TAVI patient cohort. Particularly, some studies demonstrated association between AVCS and cerebral embolization as well as acute periprocedural CVE (121, 122). Based on our results, it appears that aortic valve calcification has limited impact on cerebrovascular events as well.

In a study published by Fan et al. the authors found that patients with bicuspid aortic valve had more ischemic brain lesions after TAVI (123). In our study we found that the aortic valve calcium score was lower in patients with tricuspid valve compared to patients with bicuspid valve, however, the procedural characteristics and ILV did not differ between these two groups (Supplement Table 2).

In our study, we found that 5.3% of the patients had periprocedural stroke, which is consistent with the findings reported by Auffret and their colleagues (35). Our results indicated that periprocedural stroke was associated with predilatation and the use of alternative access routes. Predilatation was typically performed when there was significant leaflet calcification, as determined visually by the interventional cardiologist. However, there was no significant difference in AVCS between patients who underwent predilatation and those who did not. We did not observe a clear link between the number of device positioning maneuvers and the occurrence of stroke, although it's worth noting that the incidence of stroke in our study was relatively low.

Some studies found neurocognitive impairment following TAVI (46, 48), however Kahlert et al. did not find significant changes in cognitive function (111). Within a recent meta-analysis, a subgroup analysis yielded interesting findings regarding transcatheter aortic valve implantation (TAVI). Despite the emergence of new cerebral lesions following TAVI, the data revealed that 19% of participants experienced cognitive improvement, while only 7% exhibited cognitive impairment (49). Furthermore the utilization of cerebral embolic protection devices was correlated with a reduced occurrence of cognitive decline in the initial week following TAVI. Interestingly, pre-existing cognitive impairment before the TAVI procedure was associated with subsequent cognitive improvement at 6-month. It's important to note that studies with longer follow-up (46) can significantly impact the ability to identify potential associations with cognitive dysfunction compared to studies with shorter follow-up (48). Regarding to cerebral embolic protection devices according to a meta-analysis by Woldendorp they found that the use of such a devices decreased the volume of SCILs, however did not result a significant decrease in the occurrence of SCIL (48). In our study, we found that neurocognitive function remained stable throughout the one year follow-up period. We could not find any association between ILV or gliotic transformation of the procedural lesions and changes in neurocognitive function. To our knowledge, our study represents the largest patient population to date that underwent both brain MRI and underwent serial neurocognitive assessments for a year following TAVI. Furthermore, our research is the first to reveal an association between the number of device positioning maneuvers and ILV.

Procedural complications, notably CVE and SCIL, continue to pose challenges. The impact of SCIL on neurocognitive function remains a subject of debate. Hence, it is of paramount importance to identify patient and procedure related risk factors in order to attain the most favorable long-term results (79).

5.3. Microstructural white-matter changes following TAVI

In our substudy we found significant decrease of AD in 4 out of 7 white-matter ROIs (genu, body, splenium of corpus callosum and right parahippocampal cingulum). Significant MD and FA reduction were found in the body of the corpus callosum and in the splenium. We also found significant reduction of MD and RD in the left cingulate

gyrus and significant decrease of MD in the right cingulate gyrus. Overall we found significant decrease of diffusivity in 5 out of 7 WM ROIs between the post-TAVI and 6M DTI, in one ROI (splenium) we found controversial changes (reduction in AD and FA).

Among women, we observed a notably more pronounced decrease in both axial diffusivity (AD) and mean diffusivity (MD) within the body of the corpus callosum and the right cingulate gyrus. Additionally, there was a significant reduction in AD specifically within the left cingulate gyrus. Furthermore we found that ILV had a significant on DTI metrics in 3 out of 7 ROIs.

Numerous studies have shown increased AD as a sign of loss of fiber integrity linked to ageing (69, 124), cognitive impairment in Parkinson's disease (72), multiple sclerosis (125), Alzheimer's disease (71) and age-related cognitive impairment (67).

The increase in AD can be attributed to sustained axonal damage, which subsequently reduces the restriction of water diffusion along the axons. Consequently, this leads to an elevation in MD. Along with AD, though to a lesser extent, RD also increases, causing diffusion to become more isotropic, a pattern reminiscent of what is observed in chronic cerebral ischemia (64).

Regarding the specific anatomical structures we investigated, prior research has reported a significant elevation in AD within the genu of the corpus callosum in individuals with Parkinson's disease compared to control subjects (72). Additionally, increases in AD were observed in the body of the corpus callosum when comparing elderly individuals to young subjects (69) and in demented patients with Parkinson's disease when compared to those without cognitive impairment. In the two latter studies a significant increased of MD was also found. In our patient population the majority of TAVI candidates had chronic small vessel disease, we might assume an existing increase in diffusivities in line with the literature (121).

With improved cardiac output and cerebral perfusion following TAVI (116, 126), it becomes plausible that preexisting microstructural abnormalities could potentially be reversed. This reversal may lead to the normalization of abnormally elevated axial diffusivity, resulting in a net decrease in AD, as our study demonstrated in the genu and

right parahippocampal cingulum. Additionally, a net decrease in the combination of AD and MD was detected in the body of the corpus callosum. In a similar vein to our findings, previous studies reported a significant decrease in AD (127) and a significant decrease in the combination of AD and fractional anisotropy (128) in the corticospinal tract of patients with idiopathic normal pressure hydrocephalus who underwent cerebrospinal fluid derivation (127, 128). It has to be acknowledged hydrocephalus was not a prominent feature in our study group, in contrast to the other study. Nonetheless, it's important to note that both sets of patients were elderly, and they shared common characteristics such as high cardiovascular risks and associated ischemic white matter damage (129). Another potential explanation for the reduction in axial diffusivity (AD), either with or without a decrease in mean diffusivity (MD), could be attributed to several factors. These factors may include a decrease in the extracellular volume fraction, which may signify a reduction in subtle, otherwise imperceptible vasogenic white matter edema. Additionally, it could be associated with increased membrane density and a higher volume fraction of axons that have been preserved (130) since AD is not or only marginally affected in WM injury with predominant myelin degeneration. In contrast, RD experiences an increase, signifying a greater extent of unrestricted water movement perpendicular to axons (63).

Previous studies found elevated mean and radial diffusivity in the cingulate gyri when comparing Alzheimer's disease patients to healthy elderly adults (71). Similar MD and RD increases were noted in older individuals compared to younger participants in a separate study (69). Moreover, higher RD values in cingulate bundles in older subjects were linked to better prediction of cognitive performance (131). In our study, we found significant reduction in MD and RD in the left cingulate gyrus, this finding contrasts with earlier reports and may indicate a potential reorganization of damaged myelin in this region. In a small cohort, a statistically significant decrease in both mean diffusivity (MD) and radial diffusivity (RD) across the entire brain was observed, along with a notable increase in MMSE scores, after 12 months of uncomplicated carotid endarterectomy (132). These findings may lend support to our results concerning the left cingulate gyrus.

We observed a significant reduction in fractional anisotropy (FA) and, to a lesser extent in axial diffusivity (AD), along with a subtle increase in radial diffusivity (RD) in the splenium. These findings may be connected to persistent white matter (WM) deterioration that TAVI does not alleviate. They could indicate ongoing microscopic-level ischemic

WM damage, characterized by irreversible axonal loss and reactive gliosis (60). In our study, we noticed that certain changes in diffusion tensor imaging (DTI) metrics appeared to be more pronounced in female participants. Specifically, we observed a significant and more substantial reduction in axial and mean diffusivity in the body of the corpus callosum and the right cingulate gyrus among women. Additionally, there was a notably greater decrease in AD in the left cingulate gyrus in females. It's important to highlight that our study cohort exhibited significant gender differences in cardiovascular risk factors, such as lower incidence of diabetes mellitus in females, as well as differences in comorbidities, with a lower prevalence of previous myocardial infarction in female patients. However, we cannot definitively conclude whether these DTI changes are directly linked to gender or if the observed gender-specific differences in cardiovascular risk factors contribute to the alterations in DTI metrics. Given these variations in cardiovascular risks and comorbidities, one might speculate that men in our cohort may have more advanced white matter damage, resulting in less microstructural reserve, potentially leading to less favorable outcomes. Nevertheless, it's crucial to acknowledge that this explanation remains theoretical and elusive, primarily due to the limitations of our small study cohort, which do not allow us to establish causal relationships between differences in cardiovascular risks and changes in diffusivities.

In a large TAVI population with gender characteristics similar to our study (including variations in diabetes mellitus and myocardial infarction rates), short-term outcomes did not differ significantly between males and females. but males had significantly higher all-cause mortality one year after the procedure (133).

Regarding post-TAVI ischemic injury, we observed that ILV had a notable impact on changes in diffusivity metrics within three of our seven ROIs, as depicted in Figure 10. In the body of the corpus callosum, we found significant inverse correlations between ILV and all diffusivity changes (axial, mean and radial diffusivity). Notably, the most substantial difference was observed between the decrease in AD and MD in ILV groups I-II and the increase in AD and MD in ILV group III. Additionally, there was an increase in RD and a decrease in fractional anisotropy (FA) in group III, contrasting with the reduction in RD in groups I-II and a modest increase in FA in group II, although it did not reach the significance threshold. Essentially, higher ILV was associated with unfavorable microstructural changes, characterized by an overall increase in diffusivity

metrics and some loss of diffusion directionality. Furthermore, in the left cingulate gyrus, we identified a significant difference in MD reduction between ILV group II and group III. The less pronounced (though not statistically significant) decrease in FA in ILV group III, compared to the increase in FA in groups I-II, may also be linked to the absence of white matter reorganization in the presence of a higher ischemic load. In the splenium of the corpus callosum, where DTI metric changes indicated ongoing white matter degeneration, a similar effect of ILV was evident across the different ILV groups. Although a reduction in MD was observed in ILV group I, it contrasted with the slightly increased MD in group III, although the difference did not reach statistical significance following Bonferroni correction. The increase in MD and the smaller reduction in AD in ILV group III, as opposed to the more pronounced reductions in AD and MD in groups I-II, align with our earlier findings, collectively suggesting that higher ILV is associated with a lesser likelihood of reversing WM integrity loss.

The moderate improvement in several cognitive domains and the stability of overall cognitive function despite the recurrent post-TAVI ischemic brain damage in this elderly, fragile, and comorbid patient population provided evidence for the functional significance of the observed microstructural variations. In our Spearman correlation test, lower diffusivity values tended to be associated with higher cognitive scores in many regions of interest (ROIs), although statistical significance was not reached in most cases. However, notable negative correlations were observed, such as the association between radial diffusivity (RD) and language/verbal fluency in the left cingulate gyrus and the association between axial diffusivity (AD) and retrograde memory in the genu. It's essential to interpret our results cautiously, as we did not assess all white matter tracts, and the role of the studied anatomical structures in specific cognitive functions is multifaceted and goes beyond the scope of our present study.

The significance of TAVI-related cerebral ischemic injury is underscored by the finding that higher ILV was significantly associated with decreased retrograde memory and visual performance. Our findings align with a meta-analysis that demonstrated a significant positive relationship between post-TAVI cognitive dysfunction and the number of silent brain infarcts. However, it's important to note that the etiology of these infarcts is multifaceted, encompassing various patient-specific factors (such as atrial fibrillation, heart failure, and vascular disease) and procedure-specific factors (such as

pre-dilatation and valve positioning). This diversity in causes may explain the inconsistent associations with post-procedural cognitive changes reported in the literature. Additional research is required to determine the long-term impact of IBLs on cognition, particularly given that TAVI is now indicated for younger patients with better baseline cognition.

5.4. Limitations

Several limitations of the LVH remodelling study need to be acknowledged. Firstly, the lack of standardized diagnostic criteria for subclinical leaflet thrombosis (SLT) makes it challenging to compare our findings with other relevant studies. However, despite this limitation, the incidence of SLT in our study population appears consistent with previously published data (25, 133). Regarding imaging timing, the process of reverse remodelling is gradual, and SLT can develop at different time points. To address this uncertainty, we performed post-TAVI imaging at various intervals. It is important to note that our study focused on identifying more severe forms of SLT, which could potentially lead to obstruction and reduced leaflet motion. We did not specifically assess reduced leaflet motion in our investigation.

Moreover, evaluating reduced leaflet motion through CT scans poses additional challenges compared to echocardiography, primarily due to the limited temporal resolution of current CT scanners. Despite having a relatively long mean follow-up time, the composite endpoint exhibited a relatively low event rate, and we utilized all-cause mortality as one of the outcome measures. Nevertheless, our study is the first to provide evidence of the association between reverse remodelling and adverse events using CT imaging. Nonetheless, to better guide clinical practice for the diagnosis and management of SLT, further studies examining long-term outcomes are warranted (14).

We must acknowledge several limitations in the brain MRI study which analyzed 113 patients. Firstly, it was a single-center study that included 153 patients for the overall evaluation, but only 113 patients underwent brain MRI. The exclusion of patients who received a pacemaker post-TAVI or were unable to cooperate with the brain MRI may have introduced selection bias. Additionally, the proportion of patients who did not

participate in the serial neurocognitive assessment could potentially influence the observed rates of neurocognitive decline.

Furthermore, a longer follow-up duration could provide more comprehensive insights into the association between subclinical leaflet thrombosis (SCIL) and neurocognitive decline.

Moreover, the use of alternative access routes and predilatation in a limited number of patients might restrict the generalizability of our findings.

In summary, these limitations should be taken into account when interpreting the results, and further research with larger and more diverse patient populations, along with extended follow-up periods, would be valuable to gain a deeper understanding of the relationship between SCIL and neurocognitive decline (79).

Our investigation regarding the microstructural changes in the white matter has several limitations, which can be summarized as follows:

DTI is a mathematical representation of brain structure and may not always precisely reflect true brain anatomy. Factors such as noise, partial volume effects, and crossing fibers within a voxel can lead to false positive or negative results.

The interpretation of DTI indices and their relation to pathological processes remains somewhat theoretical. Having histological data would have allowed for a more direct link between changes in diffusivity and microstructural alterations. We only studied specific white matter tracts with reliable manual correction of the automated segmentation, which means other potential areas of interest were not analyzed. We did not investigate the impact of chronic cerebral microbleeds or the effects of anticoagulant and/or antiplatelet therapy on DTI indices or cognition. These aspects were beyond the scope of our study. There might be a selection bias as patients with improved general and cognitive states were more likely to participate in follow-up assessments, potentially leading to an underestimation of cognitive decline. A larger sample size would have provided more statistical power for the study.

It's important to note that the diffusion properties and their changes following TAVI have not been extensively studied, and many of the effects observed in our research may be due to factors such as aging and other pathological processes that cannot be reversed. Therefore, interpreting the reduced AD, MD, and RD is challenging, as these findings

seem to contradict numerous studies related to neurodegeneration and aging. While our results suggest potential microstructural improvements attributed to TAVI, caution is necessary since the changes could also be influenced by the clearance of subtle edema or ongoing ischemic white matter degeneration (51).

6. Conclusion

6.1. Adverse left ventricular remodelling and subclinical leaflet thrombosis following TAVI

Our study demonstrates the favorable long-term effects of TAVI on LV morphology using serial CT imaging. Our study provides insight into the interplay of HALT, reverse remodelling and clinical outcomes. We found that TAVI resulted a significant LVM regression on CT, and we demonstrated that the presence of SLT of the bioprosthetic valve and prior myocardial infarction might inhibit reverse remodelling process. Moreover, larger reverse remodelling following TAVI is associated with improved long-term prognosis and clinical outcome.

6.2. Predictors and neurological consequences of periprocedural cerebrovascular events after TAVI using MRI

We found that 92% of the patients had new cerebral ischemic lesions, however most of them were clinically silent. Balloon predilatation and the number of valve positioning attempts during the procedure were independently associated with a larger log-transformed ILV, whereas predilatation and alternative access route were associated with periprocedural stroke. The ILV was not associated with cognitive decline after TAVI.

6.3. Microstructural white-matter changes after TAVI using diffusion MRI

Significant effect of TAVI on cerebral microstructural properties was found with reduced diffusivities opposite to the general trends reported in studies of various neurodegenerative conditions and ageing, notably in women (in line with the lower cardiovascular risk revealed in females of our cohort) and lower ILV when comparing the result of the discharge brain MRI to 6M MRI results. Moreover, the overall cognitive function was maintained despite the high intrinsic ischemic load following TAVI with significant inverse relationship between ILV and cognitive scores in some domains.

7. Summary

7.1. LVH remodelling after TAVI

We investigated 117 patients with severe, symptomatic aortic stenosis who underwent CT scanning before and after TAVI procedure with a mean follow-up time of 2.6 years after TAVI. We found a significant reduction in LV mass and LVM indexed to body surface area comparing pre- vs. post-TAVI images. SLT was detected in 25.6% patients. More than 20% reduction in LVM was defined as reverse remodelling and was detected in 62.4% of the patients. SLT and prior myocardial infarction were independently associated with LV reverse remodelling after adjusting for age, gender, and traditional risk factors. Reverse remodelling was independently associated with favourable outcomes.

7.2. Predictors of CVE after TAVI

We investigated the predictors of TAVI-related ILV and periprocedural stroke in 113 consecutive patients. Neurocognitive evaluation was performed before and following TAVI at 6-month and one-year follow-up. After TAVI, 104 patients (92%) had new cerebral ischemic lesions, with 95% of these being clinically silent, while 5% of patients had stroke. In the our study, we highlighted a new predictor for ILV namely the number of attempts to position. We found that more procedural manipulations and predilatation resulted in larger log-transformed ILV on discharge MRI following TAVI. We found that predilatation and alternative acces routes were associated with stroke after TAVI.

7.3. Microstructural changes after TAVI

In a study with 78 patients who had baseline and 6-month follow-up MRIs, TAVI positively affected cerebral microstructure, reducing diffusivities, which differs from the usual trends seen in neurodegenerative and aging studies. This effect was particularly observed in women and lower ischemic lesion volume (ILV) when comparing the results of the discharge brain MRI to the 6M MRI findings. Furthermore, despite the high intrinsic ischemic burden associated with TAVI, overall cognitive function remained preserved, although there was a significant inverse relationship between ILV and cognitive scores in certain domains.

8. References

1.   Iung B, Baron G, Butchart EG, Delahaye F, Gohlke-Barwolf C, Levang OW, et al. A prospective survey of patients with valvular heart disease in Europe: The Euro Heart Survey on Valvular Heart Disease. Eur Heart J. 2003;24(13):1231-43.

2.   Heuvelman HJ, van Geldorp MW, Eijkemans MJ, Rajamannan NM, Bogers AJ, Roos-Hesselink JW, et al. Progression of aortic valve stenosis in adults: a systematic review. J Heart Valve Dis. 2012;21(4):454-62.

3.   Nathaniel S, Saligram S, Innasimuthu AL. Aortic stenosis: An update. World J Cardiol. 2010;2(6):135-9.

4.   Holmes DR, Jr., Mack MJ, Kaul S, Agnihotri A, Alexander KP, Bailey SR, et al. 2012 ACCF/AATS/SCAI/STS expert consensus document on transcatheter aortic valve replacement: developed in collabration with the American Heart Association, American Society of Echocardiography, European Association for Cardio-Thoracic Surgery, Heart Failure Society of America, Mended Hearts, Society of Cardiovascular Anesthesiologists, Society of Cardiovascular Computed Tomography, and Society for Cardiovascular Magnetic Resonance. J Thorac Cardiovasc Surg. 2012;144(3):e29-84.

5.   Liu Z, Kidney E, Bem D, Bramley G, Bayliss S, de Belder MA, et al. Transcatheter aortic valve implantation for aortic stenosis in high surgical risk patients: A systematic review and meta-analysis. PLoS One. 2018;13(5):e0196877.

6.   van Rosendael PJ, Delgado V, Bax JJ. Pacemaker implantation rate after transcatheter aortic valve implantation with early and new-generation devices: a systematic review. Eur Heart J. 2018;39(21):2003-13.

7.   Chakos A, Wilson-Smith A, Arora S, Nguyen TC, Dhoble A, Tarantini G, et al. Long term outcomes of transcatheter aortic valve implantation (TAVI): a systematic review of 5-year survival and beyond. Ann Cardiothorac Surg. 2017;6(5):432-43.

8.   Leon MB, Smith CR, Mack MJ, Makkar RR, Svensson LG, Kodali SK, et al. Transcatheter or Surgical Aortic-Valve Replacement in Intermediate-Risk Patients. N Engl J Med. 2016;374(17):1609-20.

9.   Hanzel GS, Gersh BJ. Transcatheter Aortic Valve Replacement in Low-Risk, Young Patients. Circulation. 2020;142(14):1317-9.

10.   Sundt TM, Jneid H. Guideline Update on Indications for Transcatheter Aortic Valve Implantation Based on the 2020 American College of Cardiology/American Heart

Association Guidelines for Management of Valvular Heart Disease. JAMA Cardiol. 2021;6(9):1088-9.

11.   Vahanian A, Beyersdorf F, Praz F, Milojevic M, Baldus S, Bauersachs J, et al. 2021 ESC/EACTS Guidelines for the management of valvular heart disease. Eur Heart J. 2022;43(7):561-632.

12.   Leon MB, Smith CR, Mack M, Miller DC, Moses JW, Svensson LG, et al. Transcatheter aortic-valve implantation for aortic stenosis in patients who cannot undergo surgery. N Engl J Med. 2010;363(17):1597-607.

13.   Jones DA, Tchetche D, Forrest J, Hellig F, Lansky A, Moat N. The SURTAVI study: TAVI for patients with intermediate risk. EuroIntervention. 2017;13(5):e617-e20.

14.   Szilveszter B, Oren D, Molnár L, Apor A, Nagy AI, Molnár A, et al. Subclinical leaflet thrombosis is associated with impaired reverse remodelling after transcatheter aortic valve implantation. Eur Heart J Cardiovasc Imaging. 2020;21(10):1144-51.

15.   Ali A, Patel A, Ali Z, Abu-Omar Y, Saeed A, Athanasiou T, et al. Enhanced left ventricular mass regression after aortic valve replacement in patients with aortic stenosis is associated with improved long-term survival. The Journal of Thoracic and Cardiovascular Surgery. 2011;142(2):285-91.

16.   Lindman BR, Stewart WJ, Pibarot P, Hahn RT, Otto CM, Xu K, et al. Early Regression of Severe Left Ventricular Hypertrophy After Transcatheter Aortic Valve Replacement Is Associated With Decreased Hospitalizations. JACC: Cardiovascular Interventions. 2014;7(6):662-73.

17.   Dobson LE, Musa TA, Uddin A, Fairbairn TA, Swoboda PP, Erhayiem B, et al. Acute Reverse Remodelling After Transcatheter Aortic Valve Implantation: A Link Between Myocardial Fibrosis and Left Ventricular Mass Regression. Canadian Journal of Cardiology. 2016;32(12):1411-8.

18.   Makkar RR, Fontana G, Jilaihawi H, Chakravarty T, Kofoed KF, De Backer O, et al. Possible Subclinical Leaflet Thrombosis in Bioprosthetic Aortic Valves. N Engl J Med. 2015;373(21):2015-24.

19.   Nakatani S. Subclinical leaflet thrombosis after transcatheter aortic valve implantation. Heart. 2017;103(24):1942-6.

20.   Karády J, Apor A, Nagy AI, Kolossváry M, Bartykowszki A, Szilveszter B, et al. Quantification of hypo-attenuated leaflet thickening after transcatheter aortic valve

implantation: clinical relevance of hypo-attenuated leaflet thickening volume. European Heart Journal - Cardiovascular Imaging. 2020;21(12):1395-404.

21.   Pache G, Schoechlin S, Blanke P, Dorfs S, Jander N, Arepalli CD, et al. Early hypo-attenuated leaflet thickening in balloon-expandable transcatheter aortic heart valves. Eur Heart J. 2016;37(28):2263-71.

22.   Del Trigo M, Muñoz-Garcia AJ, Wijeysundera HC, Nombela-Franco L, Cheema AN, Gutierrez E, et al. Incidence, Timing, and Predictors of Valve Hemodynamic Deterioration After Transcatheter Aortic Valve Replacement: Multicenter Registry. J Am Coll Cardiol. 2016;67(6):644-55.

23.   Issa IF, Dahl JS, Poulsen SH, Waziri F, Pedersen CT, Riber L, et al. The relation of structural valve deterioration to adverse remodelling and outcome in patients with biological heart valve prostheses. Eur Heart J Cardiovasc Imaging. 2021;22(1):82-91.

24.   Bogyi M, Schernthaner RE, Loewe C, Gager GM, Dizdarevic AM, Kronberger C, et al. Subclinical Leaflet Thrombosis After Transcatheter Aortic Valve Replacement: A Meta-Analysis. JACC Cardiovasc Interv. 2021;14(24):2643-56.

25.   Vollema EM, Kong WKF, Katsanos S, Kamperidis V, van Rosendael PJ, van der Kley F, et al. Transcatheter aortic valve thrombosis: the relation between hypo-attenuated leaflet thickening, abnormal valve haemodynamics, and stroke. Eur Heart J. 2017;38(16):1207-17.

26.   Jimenez C, Ohana M, Marchandot B, Kibler M, Carmona A, Peillex M, et al. Impact of Antithrombotic Regimen and Platelet Inhibition Extent on Leaflet Thrombosis Detected by Cardiac MDCT after Transcatheter Aortic Valve Replacement. J Clin Med. 2019;8(4).

27.   Hein M, Schoechlin S, Schulz U, Minners J, Breitbart P, Lehane C, et al. Long-Term Follow-Up of Hypoattenuated Leaflet Thickening After Transcatheter Aortic Valve Replacement. JACC: Cardiovascular Interventions. 2022;15(11):1113-22.

28.   Yanagisawa R, Tanaka M, Yashima F, Arai T, Jinzaki M, Shimizu H, et al. Early and Late Leaflet Thrombosis After Transcatheter Aortic Valve Replacement. Circ Cardiovasc Interv. 2019;12(2):e007349.

29.   Ruile P, Minners J, Breitbart P, Schoechlin S, Gick M, Pache G, et al. Medium-Term Follow-Up of Early Leaflet Thrombosis After Transcatheter Aortic Valve Replacement. JACC Cardiovasc Interv. 2018;11(12):1164-71.

30. Rashid HN, Gooley RP, Nerlekar N, Ihdayhid AR, McCormick LM, Nasis A, et al. Bioprosthetic aortic valve leaflet thrombosis detected by multidetector computed tomography is associated with adverse cerebrovascular events: a meta-analysis of observational studies. EuroIntervention. 2018;13(15):e1748-e55.

31. Nombela-Franco L, Webb JG, de Jaegere PP, Toggweiler S, Nuis RJ, Dager AE, et al. Timing, predictive factors, and prognostic value of cerebrovascular events in a large cohort of patients undergoing transcatheter aortic valve implantation. Circulation. 2012;126(25):3041-53.

32. Eggebrecht H, Schmermund A, Voigtländer T, Kahlert P, Erbel R, Mehta RH. Risk of stroke after transcatheter aortic valve implantation (TAVI): a meta-analysis of 10,037 published patients. EuroIntervention. 2012;8(1):129-38.

33. Armijo G, Nombela-Franco L, Tirado-Conte G. Cerebrovascular Events After Transcatheter Aortic Valve Implantation. Front Cardiovasc Med. 2018;5:104.

34. Winter M-P, Bartko P, Hofer F, Zbiral M, Burger A, Ghanim B, et al. Evolution of outcome and complications in TAVR: a meta-analysis of observational and randomized studies. Scientific Reports. 2020;10(1):15568.

35. Auffret V, Regueiro A, Del Trigo M, Abdul-Jawad Altisent O, Campelo-Parada F, Chiche O, et al. Predictors of Early Cerebrovascular Events in Patients With Aortic Stenosis Undergoing Transcatheter Aortic Valve Replacement. Journal of the American College of Cardiology. 2016;68(7):673-84.

36. Muntané-Carol G, Urena M, Munoz-Garcia A, Padrón R, Gutiérrez E, Regueiro A, et al. Late Cerebrovascular Events Following Transcatheter Aortic Valve Replacement. JACC: Cardiovascular Interventions. 2020;13(7):872-81.

37. Mack MJ, Leon MB, Thourani VH, Makkar R, Kodali SK, Russo M, et al. Transcatheter Aortic-Valve Replacement with a Balloon-Expandable Valve in Low-Risk Patients. N Engl J Med. 2019;380(18):1695-705.

38. Popma JJ, Deeb GM, Yakubov SJ, Mumtaz M, Gada H, O'Hair D, et al. Transcatheter Aortic-Valve Replacement with a Self-Expanding Valve in Low-Risk Patients. N Engl J Med. 2019;380(18):1706-15.

39. Arnold M, Schulz-Heise S, Achenbach S, Ott S, Dörfler A, Ropers D, et al. Embolic cerebral insults after transapical aortic valve implantation detected by magnetic resonance imaging. JACC Cardiovasc Interv. 2010;3(11):1126-32.

40.   Ghanem A, Müller A, Nähle CP, Kocurek J, Werner N, Hammerstingl C, et al. Risk and fate of cerebral embolism after transfemoral aortic valve implantation: a prospective pilot study with diffusion-weighted magnetic resonance imaging. J Am Coll Cardiol. 2010;55(14):1427-32.

41.   Rodés-Cabau J, Dumont E, Boone RH, Larose E, Bagur R, Gurvitch R, et al. Cerebral embolism following transcatheter aortic valve implantation: comparison of transfemoral and transapical approaches. J Am Coll Cardiol. 2011;57(1):18-28.

42.   Samim M, Hendrikse J, van der Worp HB, Agostoni P, Nijhoff F, Doevendans PA, et al. Silent ischemic brain lesions after transcatheter aortic valve replacement: lesion distribution and predictors. Clinical Research in Cardiology. 2015;104(5):430-8.

43.   Gu S, Coakley D, Chan D, Beska B, Singh F, Edwards R, et al. Does Transcatheter Aortic Valve Implantation for Aortic Stenosis Impact on Cognitive Function? Cardiol Rev. 2020;28(3):135-9.

44.   Ghanem A, Kocurek J, Sinning JM, Wagner M, Becker BV, Vogel M, et al. Cognitive trajectory after transcatheter aortic valve implantation. Circ Cardiovasc Interv. 2013;6(6):615-24.

45.   Auffret V, Campelo-Parada F, Regueiro A, Del Trigo M, Chiche O, Chamandi C, et al. Serial Changes in Cognitive Function Following Transcatheter Aortic Valve Replacement. J Am Coll Cardiol. 2016;68(20):2129-41.

46.   Vermeer SE, Prins ND, den Heijer T, Hofman A, Koudstaal PJ, Breteler MM. Silent brain infarcts and the risk of dementia and cognitive decline. N Engl J Med. 2003;348(13):1215-22.

47.   Azeem F, Durrani R, Zerna C, Smith EE. Silent brain infarctions and cognition decline: systematic review and meta-analysis. J Neurol. 2020;267(2):502-12.

48.   Woldendorp K, Indja B, Bannon PG, Fanning JP, Plunkett BT, Grieve SM. Silent brain infarcts and early cognitive outcomes after transcatheter aortic valve implantation: a systematic review and meta-analysis. Eur Heart J. 2021;42(10):1004-15.

49.   Ghezzi ES, Ross TJ, Davis D, Psaltis PJ, Loetscher T, Keage HAD. Meta-Analysis of Prevalence and Risk Factors for Cognitive Decline and Improvement After Transcatheter Aortic Valve Implantation. Am J Cardiol. 2020;127:105-12.

50.   Eggermont LH, de Boer K, Muller M, Jaschke AC, Kamp O, Scherder EJ. Cardiac disease and cognitive impairment: a systematic review. Heart. 2012;98(18):1334-40.

51.   Varga A, Gyebnár G, Suhai FI, Nagy AI, Kozák LR, Póka C, et al. Microstructural alterations measured by diffusion tensor imaging following transcatheter aortic valve replacement and their association with cerebral ischemic injury and cognitive function - a prospective study. Neuroradiology. 2022;64(12):2343-56.

52.   Blanke P, Weir-McCall JR, Achenbach S, Delgado V, Hausleiter J, Jilaihawi H, et al. Computed Tomography Imaging in the Context of Transcatheter Aortic Valve Implantation (TAVI)/Transcatheter Aortic Valve Replacement (TAVR): An Expert Consensus Document of the Society of Cardiovascular Computed Tomography. JACC Cardiovasc Imaging. 2019;12(1):1-24.

53.   Delgado V, Ng AC, van de Veire NR, van der Kley F, Schuijf JD, Tops LF, et al. Transcatheter aortic valve implantation: role of multi-detector row computed tomography to evaluate prosthesis positioning and deployment in relation to valve function. Eur Heart J. 2010;31(9):1114-23.

54.   Ng AC, Delgado V, van der Kley F, Shanks M, van de Veire NR, Bertini M, et al. Comparison of aortic root dimensions and geometries before and after transcatheter aortic valve implantation by 2- and 3-dimensional transesophageal echocardiography and multislice computed tomography. Circ Cardiovasc Imaging. 2010;3(1):94-102.

55.   Blanke P, Schoepf UJ, Leipsic JA. CT in transcatheter aortic valve replacement. Radiology. 2013;269(3):650-69.

56.   Klein R, Ametepe ES, Yam Y, Dwivedi G, Chow BJ. Cardiac CT assessment of left ventricular mass in mid-diastasis and its prognostic value. European Heart Journal - Cardiovascular Imaging. 2017;18(1):95-102.

57.   Raman SV, Shah M, McCarthy B, Garcia A, Ferketich AK. Multi-detector row cardiac computed tomography accurately quantifies right and left ventricular size and function compared with cardiac magnetic resonance. Am Heart J. 2006;151(3):736-44.

58.   Foppa M, Duncan BB, Rohde LE. Echocardiography-based left ventricular mass estimation. How should we define hypertrophy? Cardiovasc Ultrasound. 2005;3:17.

59.   Maffei E, Messalli G, Martini C, Nieman K, Catalano O, Rossi A, et al. Left and right ventricle assessment with Cardiac CT: validation study vs. Cardiac MR. Eur Radiol. 2012;22(5):1041-9.

60.   Basser PJ, Pierpaoli C. Microstructural and physiological features of tissues elucidated by quantitative-diffusion-tensor MRI. J Magn Reson B. 1996;111(3):209-19.

61. Le Bihan D, Mangin JF, Poupon C, Clark CA, Pappata S, Molko N, et al. Diffusion tensor imaging: concepts and applications. J Magn Reson Imaging. 2001;13(4):534-46.

62. Wycliffe ND, Holshouser BA, Bartnik-Olson B, Ashwal S. 12 - Pediatric Neuroimaging. In: Swaiman KF, Ashwal S, Ferriero DM, Schor NF, Finkel RS, Gropman AL, et al., editors. Swaiman's Pediatric Neurology (Sixth Edition): Elsevier; 2017. p. 78-86.

63. Song SK, Yoshino J, Le TQ, Lin SJ, Sun SW, Cross AH, et al. Demyelination increases radial diffusivity in corpus callosum of mouse brain. Neuroimage. 2005;26(1):132-40.

64. Song SK, Sun SW, Ju WK, Lin SJ, Cross AH, Neufeld AH. Diffusion tensor imaging detects and differentiates axon and myelin degeneration in mouse optic nerve after retinal ischemia. Neuroimage. 2003;20(3):1714-22.

65. Beaulieu C. The basis of anisotropic water diffusion in the nervous system - a technical review. NMR Biomed. 2002;15(7-8):435-55.

66. Sullivan EV, Rohlfing T, Pfefferbaum A. Quantitative fiber tracking of lateral and interhemispheric white matter systems in normal aging: relations to timed performance. Neurobiol Aging. 2010;31(3):464-81.

67. Voineskos AN, Rajji TK, Lobaugh NJ, Miranda D, Shenton ME, Kennedy JL, et al. Age-related decline in white matter tract integrity and cognitive performance: a DTI tractography and structural equation modeling study. Neurobiol Aging. 2012;33(1):21-34.

68. Alexander AL, Lee JE, Lazar M, Field AS. Diffusion tensor imaging of the brain. Neurotherapeutics. 2007;4(3):316-29.

69. Burzynska AZ, Preuschhof C, Bäckman L, Nyberg L, Li SC, Lindenberger U, et al. Age-related differences in white matter microstructure: region-specific patterns of diffusivity. Neuroimage. 2010;49(3):2104-12.

70. Gyebnár G, Szabó Á, Sirály E, Fodor Z, Sákovics A, Salacz P, et al. What can DTI tell about early cognitive impairment? - Differentiation between MCI subtypes and healthy controls by diffusion tensor imaging. Psychiatry Res Neuroimaging. 2018;272:46-57.

71.   Mayo CD, Garcia-Barrera MA, Mazerolle EL, Ritchie LJ, Fisk JD, Gawryluk JR. Relationship Between DTI Metrics and Cognitive Function in Alzheimer's Disease. Front Aging Neurosci. 2018;10:436.

72.   Bledsoe IO, Stebbins GT, Merkitch D, Goldman JG. White matter abnormalities in the corpus callosum with cognitive impairment in Parkinson disease. Neurology. 2018;91(24):e2244-e55.

73.   Xiong Y, Sui Y, Xu Z, Zhang Q, Karaman MM, Cai K, et al. A Diffusion Tensor Imaging Study on White Matter Abnormalities in Patients with Type 2 Diabetes Using Tract-Based Spatial Statistics. AJNR Am J Neuroradiol. 2016;37(8):1462-9.

74.   Karády J, Apor A, Nagy AI, Kolossváry M, Bartykowszki A, Szilveszter B, et al. Quantification of hypo-attenuated leaflet thickening after transcatheter aortic valve implantation: clinical relevance of hypo-attenuated leaflet thickening volume. Eur Heart J Cardiovasc Imaging. 2020;21(12):1395-404.

75.   Pawade T, Clavel M-A, Tribouilloy C, Dreyfus J, Mathieu T, Tastet L, et al. Computed Tomography Aortic Valve Calcium Scoring in Patients With Aortic Stenosis. Circulation: Cardiovascular Imaging. 2018;11(3):e007146.

76.   Zannad F, Stough WG, Pitt B, Cleland JG, Adams KF, Geller NL, et al. Heart failure as an endpoint in heart failure and non-heart failure cardiovascular clinical trials: the need for a consensus definition. Eur Heart J. 2008;29(3):413-21.

77.   Kappetein AP, Head SJ, Généreux P, Piazza N, van Mieghem NM, Blackstone EH, et al. Updated standardized endpoint definitions for transcatheter aortic valve implantation: the Valve Academic Research Consortium-2 consensus document. Eur Heart J. 2012;33(19):2403-18.

78.   Généreux P, Piazza N, Alu MC, Nazif T, Hahn RT, Pibarot P, et al. Valve Academic Research Consortium 3: Updated Endpoint Definitions for Aortic Valve Clinical Research. Journal of the American College of Cardiology. 2021;77(21):2717-46.

79.   Suhai FI, Varga A, Szilveszter B, Nagy-Vecsey M, Apor A, Nagy AI, et al. Predictors and neurological consequences of periprocedural cerebrovascular events following transcatheter aortic valve implantation with self-expanding valves. Front Cardiovasc Med. 2022;9:951943.

80.   Leemans A, Jeurissen B, Sijbers J, Jones DK, editors. ExploreDTI: a graphical toolbox for processing, analyzing, and visualizing diffusion MR data2009.

81.　　Jezzard P, Barnett AS, Pierpaoli C. Characterization of and correction for eddy current artifacts in echo planar diffusion imaging. Magn Reson Med. 1998;39(5):801-12.

82.　　Chang LC, Jones DK, Pierpaoli C. RESTORE: robust estimation of tensors by outlier rejection. Magn Reson Med. 2005;53(5):1088-95.

83.　　Bezinque A, Moriarity A, Farrell C, Peabody H, Noyes SL, Lane BR. Determination of Prostate Volume: A Comparison of Contemporary Methods. Acad Radiol. 2018;25(12):1582-7.

84.　　Mathuranath PS, Nestor PJ, Berrios GE, Rakowicz W, Hodges JR. A brief cognitive test battery to differentiate Alzheimer's disease and frontotemporal dementia. Neurology. 2000;55(11):1613-20.

85.　　Still S, Szerlip M, Mack M. TAVR Vs. SAVR in Intermediate-Risk Patients: What Influences Our Choice of Therapy. Curr Cardiol Rep. 2018;20(10):82.

86.　　Rogers T, Thourani VH, Waksman R. Transcatheter Aortic Valve Replacement in Intermediate- and Low-Risk Patients. J Am Heart Assoc. 2018;7(10).

87.　　Dangas GD, Weitz JI, Giustino G, Makkar R, Mehran R. Prosthetic Heart Valve Thrombosis. J Am Coll Cardiol. 2016;68(24):2670-89.

88.　　Spartera M, Ancona F, Barletta M, Rosa I, Stella S, Marini C, et al. Echocardiographic features of post-transcatheter aortic valve implantation thrombosis and endocarditis. Echocardiography. 2018;35(3):337-45.

89.　　Sondergaard L, De Backer O, Kofoed KF, Jilaihawi H, Fuchs A, Chakravarty T, et al. Natural history of subclinical leaflet thrombosis affecting motion in bioprosthetic aortic valves. Eur Heart J. 2017;38(28):2201-7.

90.　　Garcia S, Fukui M, Dworak MW, Okeson BK, Garberich R, Hashimoto G, et al. Clinical Impact of Hypoattenuating Leaflet Thickening After Transcatheter Aortic Valve Replacement. Circ Cardiovasc Interv. 2022;15(3):e011480.

91.　　Chakravarty T, Søndergaard L, Friedman J, De Backer O, Berman D, Kofoed KF, et al. Subclinical leaflet thrombosis in surgical and transcatheter bioprosthetic aortic valves: an observational study. Lancet. 2017;389(10087):2383-92.

92.　　Ruile P, Minners J, Schoechlin S, Pache G, Hochholzer W, Blanke P, et al. Impact of the type of transcatheter heart valve on the incidence of early subclinical leaflet thrombosis. Eur J Cardiothorac Surg. 2018;53(4):778-83.

93.   Magalhaes MA, Koifman E, Torguson R, Minha S, Gai J, Kiramijyan S, et al. Outcome of Left-Sided Cardiac Remodeling in Severe Aortic Stenosis Patients Undergoing Transcatheter Aortic Valve Implantation. Am J Cardiol. 2015;116(4):595-603.

94.   Dobson LE, Musa TA, Uddin A, Fairbairn TA, Swoboda PP, Erhayiem B, et al. Acute Reverse Remodelling After Transcatheter Aortic Valve Implantation: A Link Between Myocardial Fibrosis and Left Ventricular Mass Regression. Can J Cardiol. 2016;32(12):1411-8.

95.   Nucifora G, Tantiongco JP, Crouch G, Bennetts J, Sinhal A, Tully PJ, et al. Changes of left ventricular mechanics after trans-catheter aortic valve implantation and surgical aortic valve replacement for severe aortic stenosis: A tissue-tracking cardiac magnetic resonance study. Int J Cardiol. 2017;228:184-90.

96.   Fairbairn TA, Steadman CD, Mather AN, Motwani M, Blackman DJ, Plein S, et al. Assessment of valve haemodynamics, reverse ventricular remodelling and myocardial fibrosis following transcatheter aortic valve implantation compared to surgical aortic valve replacement: a cardiovascular magnetic resonance study. Heart. 2013;99(16):1185-91.

97.   Mehdipoor G, Chen S, Chatterjee S, Torkian P, Ben-Yehuda O, Leon MB, et al. Cardiac structural changes after transcatheter aortic valve replacement: systematic review and meta-analysis of cardiovascular magnetic resonance studies. J Cardiovasc Magn Reson. 2020;22(1):41.

98.   Makkar RR, Blanke P, Leipsic J, Thourani V, Chakravarty T, Brown D, et al. Subclinical Leaflet Thrombosis in Transcatheter and Surgical Bioprosthetic Valves: PARTNER 3 Cardiac Computed Tomography Substudy. J Am Coll Cardiol. 2020;75(24):3003-15.

99.   Koren MJ, Devereux RB, Casale PN, Savage DD, Laragh JH. Relation of left ventricular mass and geometry to morbidity and mortality in uncomplicated essential hypertension. Ann Intern Med. 1991;114(5):345-52.

100.   Levy D. Clinical significance of left ventricular hypertrophy: insights from the Framingham Study. J Cardiovasc Pharmacol. 1991;17 Suppl 2:S1-6.

101.   Christakis GT, Joyner CD, Morgan CD, Fremes SE, Buth KJ, Sever JY, et al. Left ventricular mass regression early after aortic valve replacement. Ann Thorac Surg. 1996;62(4):1084-9.

102.   Treibel TA, Kozor R, Schofield R, Benedetti G, Fontana M, Bhuva AN, et al. Reverse Myocardial Remodeling Following Valve Replacement in Patients With Aortic Stenosis. J Am Coll Cardiol. 2018;71(8):860-71.

103.   Lindman BR, Stewart WJ, Pibarot P, Hahn RT, Otto CM, Xu K, et al. Early regression of severe left ventricular hypertrophy after transcatheter aortic valve replacement is associated with decreased hospitalizations. JACC Cardiovasc Interv. 2014;7(6):662-73.

104.   Athappan G, Patvardhan E, Tuzcu EM, Svensson LG, Lemos PA, Fraccaro C, et al. Incidence, predictors, and outcomes of aortic regurgitation after transcatheter aortic valve replacement: meta-analysis and systematic review of literature. J Am Coll Cardiol. 2013;61(15):1585-95.

105.   Puls M, Beuthner BE, Topci R, Vogelgesang A, Bleckmann A, Sitte M, et al. Impact of myocardial fibrosis on left ventricular remodelling, recovery, and outcome after transcatheter aortic valve implantation in different haemodynamic subtypes of severe aortic stenosis. Eur Heart J. 2020;41(20):1903-14.

106.   Vizzardi E, D'Aloia A, Fiorina C, Bugatti S, Parrinello G, De Carlo M, et al. Early regression of left ventricular mass associated with diastolic improvement after transcatheter aortic valve implantation. J Am Soc Echocardiogr. 2012;25(10):1091-8.

107.   Abdelghani M, Tateishi H, Miyazaki Y, Cavalcante R, Soliman OII, Tijssen JG, et al. Angiographic assessment of aortic regurgitation by video-densitometry in the setting of TAVI: Echocardiographic and clinical correlates. Catheter Cardiovasc Interv. 2017;90(4):650-9.

108.   Kuneman JH, Singh GK, Hansson NC, Fusini L, Poulsen SH, Fortuni F, et al. Subclinical leaflet thrombosis after transcatheter aortic valve implantation: no association with left ventricular reverse remodeling at 1-year follow-up. Int J Cardiovasc Imaging. 2022;38(3):695-705.

109.   Bosmans J, Bleiziffer S, Gerckens U, Wenaweser P, Brecker S, Tamburino C, et al. The Incidence and Predictors of Early- and Mid-Term Clinically Relevant

Neurological Events After Transcatheter Aortic Valve Replacement in Real-World Patients. Journal of the American College of Cardiology. 2015;66(3):209-17.

110. De Carlo M, Liga R, Migaleddu G, Scatturin M, Spaccarotella C, Fiorina C, et al. Evolution, Predictors, and Neurocognitive Effects of Silent Cerebral Embolism During Transcatheter Aortic Valve Replacement. JACC Cardiovasc Interv. 2020;13(11):1291-300.

111. Kahlert P, Knipp SC, Schlamann M, Thielmann M, Al-Rashid F, Weber M, et al. Silent and apparent cerebral ischemia after percutaneous transfemoral aortic valve implantation: a diffusion-weighted magnetic resonance imaging study. Circulation. 2010;121(7):870-8.

112. Kajio K, Mizutani K, Hara M, Nakao M, Okai T, Ito A, et al. Self-expandable transcatheter aortic valve replacement is associated with frequent periprocedural stroke detected by diffusion-weighted magnetic resonance imaging. J Cardiol. 2019;74(1):27-33.

113. Kleiman NS, Maini BJ, Reardon MJ, Conte J, Katz S, Rajagopal V, et al. Neurological Events Following Transcatheter Aortic Valve Replacement and Their Predictors: A Report From the CoreValve Trials. Circ Cardiovasc Interv. 2016;9(9).

114. Mastoris I, Schoos MM, Dangas GD, Mehran R. Stroke after transcatheter aortic valve replacement: incidence, risk factors, prognosis, and preventive strategies. Clin Cardiol. 2014;37(12):756-64.

115. Van Mieghem NM, El Faquir N, Rahhab Z, Rodríguez-Olivares R, Wilschut J, Ouhlous M, et al. Incidence and predictors of debris embolizing to the brain during transcatheter aortic valve implantation. JACC Cardiovasc Interv. 2015;8(5):718-24.

116. Vlastra W, van den Boogert TPW, Krommenhoek T, Bronzwaer AGT, Mutsaerts H, Achterberg HC, et al. Aortic valve calcification volumes and chronic brain infarctions in patients undergoing transcatheter aortic valve implantation. Int J Cardiovasc Imaging. 2019;35(11):2123-33.

117. Tchetche D, Farah B, Misuraca L, Pierri A, Vahdat O, Lereun C, et al. Cerebrovascular Events Post-Transcatheter Aortic Valve Replacement in a Large Cohort of Patients: A FRANCE-2 Registry Substudy. JACC: Cardiovascular Interventions. 2014;7(10):1138-45.

118.   Nuis R-J, Van Mieghem NM, Schultz CJ, Moelker A, van der Boon RM, van Geuns RJ, et al. Frequency and Causes of Stroke During or After Transcatheter Aortic Valve Implantation. The American Journal of Cardiology. 2012;109(11):1637-43.

119.   Lu H, Monney P, Hullin R, Fournier S, Roguelov C, Eeckhout E, et al. Transcarotid Access Versus Transfemoral Access for Transcatheter Aortic Valve Replacement: A Systematic Review and Meta-Analysis. Front Cardiovasc Med. 2021;8:687168.

120.   Bjursten H, Norrving B, Ragnarsson S. Late stroke after transcatheter aortic valve replacement: a nationwide study. Scientific Reports. 2021;11(1):9593.

121.   Doerner J, Kupczyk PA, Wilsing M, Luetkens JA, Storm K, Fimmers R, et al. Cerebral white matter lesion burden is associated with the degree of aortic valve calcification and predicts peri-procedural cerebrovascular events in patients undergoing transcatheter aortic valve implantation (TAVI). Catheter Cardiovasc Interv. 2018;91(4):774-82.

122.   Aggarwal SK, Delahunty Rn N, Menezes LJ, Perry R, Wong B, Reinthaler M, et al. Patterns of solid particle embolization during transcatheter aortic valve implantation and correlation with aortic valve calcification. J Interv Cardiol. 2018;31(5):648-54.

123.   Fan J, Fang X, Liu C, Zhu G, Hou Cody R, Jiang J, et al. Brain Injury After Transcatheter Replacement of Bicuspid Versus Tricuspid Aortic Valves. Journal of the American College of Cardiology. 2020;76(22):2579-90.

124.   Zavaliangos-Petropulu A, Nir TM, Thomopoulos SI, Reid RI, Bernstein MA, Borowski B, et al. Diffusion MRI Indices and Their Relation to Cognitive Impairment in Brain Aging: The Updated Multi-protocol Approach in ADNI3. Front Neuroinform. 2019;13:2.

125.   Llufriu S, Blanco Y, Martinez-Heras E, Casanova-Molla J, Gabilondo I, Sepulveda M, et al. Influence of corpus callosum damage on cognition and physical disability in multiple sclerosis: a multimodal study. PLoS One. 2012;7(5):e37167.

126.   Tsuchiya S, Matsumoto Y, Suzuki H, Takanami K, Kikuchi Y, Takahashi J, et al. Transcatheter aortic valve implantation and cognitive function in elderly patients with severe aortic stenosis. EuroIntervention. 2020;15(18):e1580-e7.

127.   Kamiya K, Hori M, Irie R, Miyajima M, Nakajima M, Kamagata K, et al. Diffusion imaging of reversible and irreversible microstructural changes within the

corticospinal tract in idiopathic normal pressure hydrocephalus. Neuroimage Clin. 2017;14:663-71.

128. Jurcoane A, Keil F, Szelenyi A, Pfeilschifter W, Singer OC, Hattingen E. Directional diffusion of corticospinal tract supports therapy decisions in idiopathic normal-pressure hydrocephalus. Neuroradiology. 2014;56(1):5-13.

129. Israelsson H, Larsson J, Eklund A, Malm J. Risk factors, comorbidities, quality of life, and complications after surgery in idiopathic normal pressure hydrocephalus: review of the INPH-CRasH study. Neurosurg Focus. 2020;49(4):E8.

130. Sen PN, Basser PJ. A model for diffusion in white matter in the brain. Biophys J. 2005;89(5):2927-38.

131. Davis SW, Dennis NA, Buchler NG, White LE, Madden DJ, Cabeza R. Assessing the effects of age on long white matter tracts using diffusion tensor tractography. Neuroimage. 2009;46(2):530-41.

132. Porcu M, Cocco L, Cau R, Suri JS, Mannelli L, Puig J, et al. Mid-term effects of carotid endarterectomy on cognition and white matter status evaluated by whole brain diffusion tensor imaging metrics: A preliminary analysis. Eur J Radiol. 2022;151:110314.

133. Yousif N, Obeid S, Binder R, Denegri A, Shahin M, Templin C, et al. Impact of gender on outcomes after transcatheter aortic valve implantation. J Geriatr Cardiol. 2018;15(6):394-400.

134. Marwan M, Mekkhala N, Göller M, Röther J, Bittner D, Schuhbaeck A, et al. Leaflet thrombosis following transcatheter aortic valve implantation. J Cardiovasc Comput Tomogr. 2018;12(1):8-13

9. Bibliography of the candidate's publications

9.1. Publication related to the present thesis

1. Bálint Szilveszter, Daniel Oren, Levente Molnár, Astrid Apor, Anikó I Nagy, Andrea Molnár, Borbála Vattay, Márton Kolossváry, Júlia Karády, Andrea Bartykowszki, Ádám L Jermendy, **Ferenc I Suhai**, Alexisz Panajotu, Pál Maurovich-Horvat, Béla Merkely, Subclinical leaflet thrombosis is associated with impaired reverse remodelling after transcatheter aortic valve implantation, European Heart Journal - Cardiovascular Imaging, Volume 21, Issue 10, October 2020, Pages 1144–1151 **(IF: 4,841)**

2. **Suhai FI**, Varga A, Szilveszter B, Nagy-Vecsey M, Apor A, Nagy AI, Kolossváry M, Karády J, Bartykowszki A, Molnár L, Jermendy ÁL, Panajotu A, Maurovich-Horvat P, Merkely B. Predictors and neurological consequences of periprocedural cerebrovascular events following transcatheter aortic valve implantation with self-expanding valves. Front Cardiovasc Med. 2022 Oct 5;9:951943. **(IF: 5,05).**

3. Varga A, Gyebnár G, **Suhai FI**, Nagy AI, Kozák LR, Póka CÁ, Turáni MF, Borzsák S, Apor A, Bartykowszki A, Szilveszter B, Kolossváry M, Maurovich-Horvat P, Merkely B. Microstructural alterations measured by diffusion tensor imaging following transcatheter aortic valve replacement and their association with cerebral ischemic injury and cognitive function - a prospective study. Neuroradiology. 2022 Dec;64(12):2343-2356. **(IF: 2,98)**

9.2. Publications not related to the thesis

1. Szilveszter B, Nagy AI, Vattay B, Apor A, Kolossváry M, Bartykowszki A, Simon J, Drobni ZD, Tóth A, **Suhai FI**, Merkely B, Maurovich-Horvat P. Left ventricular and atrial strain imaging with cardiac computed tomography: Validation against echocardiography. J Cardiovasc Comput Tomogr. 2020 Jul-Aug;14(4):363-369.

2. Karády J, Apor A, Nagy AI, Kolossváry M, Bartykowszki A, Szilveszter B, Simon J, Molnár L, Jermendy ÁL, Panajotu A, **Suhai FI**, Varga A, Rajani R, Maurovich-Horvat P, Merkely B. Quantification of hypo-attenuated leaflet thickening after transcatheter aortic valve implantation: clinical relevance of hypo-attenuated leaflet thickening volume. Eur Heart J Cardiovasc Imaging. 2020 Dec 1;21(12):1395-1404.

3. Vágó H, Szabó L, Dohy Z, Czimbalmos C, Tóth A, Suhai FI, Bárczi G, Gyarmathy VA, Becker D, Merkely B. Early cardiac magnetic resonance imaging in troponin-positive acute chest pain and non-obstructed coronary arteries Heart. 2020 Jul;106(13):992-1000.

4. Dohy Z, Vereckei A, Horvath V, Czimbalmos C, Szabo L, Toth A, **Suhai FI**, Csecs I, Becker D, Merkely B, Vago H. How are ECG parameters related to cardiac magnetic resonance images? Electrocardiographic predictors of left ventricular hypertrophy and myocardial fibrosis in hypertrophic cardiomyopathy. Ann Noninvasive Electrocardiol. 2020 Sep;25(5):e12763.

5. Maurovich-Horvat P, Károlyi M, Horváth T, Szilveszter B, Bartykowszki A, Jermendy ÁL, Panajotu A, Celeng C, **Suhai FI**, Major GP, Csobay-Novák C, Hüttl K, Merkely B. Esmolol is noninferior to metoprolol in achieving a target heart rate of 65 beats/min in patients referred to coronary CT angiography: a randomized controlled clinical trial. J Cardiovasc Comput Tomogr. 2015 Mar-Apr;9(2):139-45. doi: 10.1016/j.jcct.2015.02.001. Epub 2015 Feb 14. PMID: 25819196.

6. Csecs I, Czimbalmos C, **Suhai FI**, Mikle R, Mirzahosseini A, Dohy Z, Szűcs A, Kiss AR, Simor T, Tóth A, Merkely B, Vágó H. Left and right ventricular parameters corrected with threshold-based quantification method in a normal cohort analyzed by three independent observers with various training-degree. Int J Cardiovasc Imaging. 2018 Jul;34(7):1127-1133.

7. Czimbalmos C, Csecs I, Toth A, Kiss O, **Suhai FI**, Sydo N, Dohy Z, Apor A, Merkely B, Vago H. The demanding grey zone: Sport indices by cardiac magnetic resonance imaging differentiate hypertrophic cardiomyopathy from athlete's heart. PLoS One. 2019 Feb 14;14(2):e0211624.

8. Czimbalmos C, Csecs I, Dohy Z, Toth A, **Suhai FI**, Müssigbrodt A, Kiss O, Geller L, Merkely B, Vago H. Cardiac magnetic resonance based deformation imaging: role of feature tracking in athletes with suspected arrhythmogenic right ventricular cardiomyopathy. Int J CardiovascImaging. 2019 Mar;35(3):529-538.

9. Csecs I, Czimbalmos C, Toth A, Dohy Z, **Suhai IF**, Szabo L, Kovacs A, Lakatos B, Sydo N, Kheirkhahan M, Peritz D, Kiss O, Merkely B, Vago H. The impact of sex, age and training on biventricular cardiac adaptation in healthy adult and adolescent athletes: Cardiac magnetic resonance imaging study. Eur J Prev Cardiol. 2020 Mar;27(5):540-549.

10. Székely M, Ruttkay T, **Suhai FI**, Bóna Á, Merkely B, Székely L. Minimally invasive apical cannulation and cannula design for short-term mechanical circulatory support devices. BMC Cardiovasc Disord. 2022 Sep 4;22(1):395.

11. Apor A, Bartykowszki A, Szilveszter B, Varga A, **Suhai FI**, Manouras A, Molnár L, Jermendy ÁL, Panajotu A, Turáni MF, Papp R, Karády J, Kolossváry M, Kováts T, Maurovich-Horvat P, Merkely B, Nagy AI. Subclinical leaflet thrombosis after transcatheter aortic valve implantation is associated with silent brain injury on brain magnetic resonance imaging. Eur Heart J Cardiovasc Imaging. 2022 Nov 17;23(12):1584-1595.

12. Szűcs A, Kiss AR, **Suhai FI**, Tóth A, Gregor Z, Horváth M, Czimbalmos C, Csécs I, Dohy Z, Szabó LE, Merkely B, Vágó H. The effect of contrast agents

on left ventricular parameters calculated by a threshold-based software module: does it truly matter? Int J Cardiovasc Imaging. 2019 Sep;35(9):1683-1689.

13. Maurovich-Horvat P, **Suhai FI**, Czimbalmos C, Tóth A, Becker D, Kiss E, Ferencik M, Hoffmann U, Vagó H, Merkely B. Coronary Artery Manifestation of Ormond Disease: The "Mistletoe Sign". Radiology. 2016 Aug 22:160644.

14. Vecsey-Nagy M, Jermendy ÁL, Kolossváry M, Vattay B, Boussoussou M, **Suhai FI**, Panajotu A, Csőre J, Borzsák S, Fontanini DM, Csobay-Novák C, Merkely B, Maurovich-Horvat P, Szilveszter B. Heart Rate-Dependent Degree of Motion Artifacts in Coronary CT Angiography Acquired by a Novel Purpose-Built Cardiac CT Scanner. J Clin Med. 2022 Jul 26;11(15):4336.

15. Szabó L, Juhász V, Dohy Z, Fogarasi C, Kovács A, Lakatos BK, Kiss O, Sydó N, Csulak E, **Suhai FI**, Hirschberg K, Becker D, Merkely B, Vágó H. Is cardiac involvement prevalent in highly trained athletes after SARS-CoV-2 infection? A cardiac magnetic resonance study using sex-matched and age-matched controls Br J Sports Med. 2022 May;56(10):553-560.

16. Vecsey-Nagy M, Jermendy ÁL, **Suhai FI**, Panajotu A, Csőre J, Borzsák S, Fontanini DM, Kolossváry M, Vattay B, Boussoussou M, Csobay-Novák C, Merkely B, Maurovich-Horvat P, Szilveszter B. Model-based adaptive filter for a dedicated cardiovascular CT scanner: Assessment of image noise, sharpness and quality.
Eur J Radiol. 2021 Dec;145:110032.

17. Szűcs A, Kiss AR, Gregor Z, Horváth M, Tóth A, Dohy Z, Szabó LE, **Suhai FI**, Merkely B, Vágó H. Changes in strain parameters at different deterioration levels of left ventricular function: A cardiac magnetic resonance feature-tracking study of patients with left ventricular noncompaction. Int J Cardiol. 2021 May 15;331:124-130.

18. Budai A*, **Suhai FI***, Csorba K, Toth A, Szabo L, Vago H, Merkely B. Fully automatic segmentation of right and left ventricle on short-axis cardiac MRI

images

Comput Med Imaging Graph. 2020 Oct;85:101786.

19. Tokodi M, Staub L, Budai Á, Lakatos BK, Csákvári M, **Suhai FI**, Szabó L, Fábián A, Vágó H, Tősér Z, Merkely B, Kovács A. Partitioning the Right Ventricle Into 15 Segments and Decomposing Its Motion Using 3D Echocardiography-Based Models: The Updated ReVISION Method. Front Cardiovasc Med. 2021 Mar 4;8:622118.

20. Ádám Budai; **Ferenc Imre Suhai**; Kristof Csorba; Zsofia Dohy; Liliana Szabo; Bela Merkely; Hajnalka Vago. Automated Classification of Left Ventricular Hypertrophy on Cardiac MRI. Applied Sciences Appl. Sci. 2022, 12, 4151.

21. Szegedi N, **Suhai IF**, Perge P, Salló Z, Hartyánszky I, Merkely B, Gellér L J Atrio-esophageal fistula clinically presented as pericardial-esophageal fistula. Interv Card Electrophysiol. 2021 Sep;61(3):623-624.

22. Székely R, **Suhai FI**, Karlinger K, Baksa G, Szabaczki B, Bárány L, Pölöskei G, Rácz G, Wagner Ö, Merkely B, Ruttkay T. Human Cadaveric Artificial Lung Tumor-Mimic Training Model. Pathol Oncol Res. 2021 Apr 26;27:630459.

23. Vattay B, Borzsák S, Boussoussou M, Vecsey-Nagy M, Jermendy ÁL, **Suhai FI**, Maurovich-Horvat P, Merkely B, Kolossváry M, Szilveszter B. Association between coronary plaque volume and myocardial ischemia detected by dynamic perfusion CT imaging. Front Cardiovasc Med. 2022 Sep 8;9:974805.

24. Vago H, Czimbalmos C, Papp R, Szabo L, Toth A, Dohy Z, Csecs I, **Suhai F**, Kosztin A, Molnar L, Geller L, Merkely B. Biventricular pacing during cardiac magnetic resonance imaging. Europace. 2020 Jan 1;22(1):117-124.

25. Dohy Z, Szabo L, Toth A, Czimbalmos C, Horvath R, Horvath V, **Suhai FI**, Geller L, Merkely B, Vago H. Prognostic significance of cardiac magnetic resonance-based markers in patients with hypertrophic cardiomyopathy. Int J Cardiovasc Imaging. 2021 Jun;37(6):2027-2036.

26. Șulea CM, Lakatos B, Kovács A, Benke K, **Suhai FI**, Csulak E, Merkel E, Nagy B, Hartyánszky I, Merkely B, Szabolcs Z, Pólos M. Blood-filled cyst of the tricuspid valve: Multiple cardiac disorders, one surgical case. J Card Surg. 2022 Jan;37(1):245-248.

27. Csulak E, Petrov Á, Kováts T, Tokodi M, Lakatos B, Kovács A, Staub L, **Suhai FI**, Szabó EL, Dohy Z, Vágó H, Becker D, Müller V, Sydó N, Merkely B. The Impact of COVID-19 on the Preparation for the Tokyo Olympics: A Comprehensive Performance Assessment of Top Swimmers. Int J Environ Res Public Health. 2021 Sep 16;18(18):9770.

28. Dohy Z, Szabo L, Pozsonyi Z, Csecs I, Toth A, **Suhai FI**, Czimbalmos C, Szucs A, Kiss AR, Becker D, Merkely B, Vago H. Potential clinical relevance of cardiac magnetic resonance to diagnose cardiac light chain amyloidosis. PLoS One. 2022 Jun 13;17(6):e0269807.

29. Csőre J, **Suhai FI**, Gyánó M, Pataki ÁA, Juhász G, Vecsey-Nagy M, Pál D, Fontanini DM, Bérczi Á, Csobay-Novák C. Quiescent-Interval Single-Shot Magnetic Resonance Angiography May Outperform Carbon-Dioxide Digital Subtraction Angiography in Chronic Lower Extremity Peripheral Arterial Disease. J Clin Med. 2022 Aug 1;11(15):4485.

30. Jermendy, G., Kolossváry, M., Dudás, I., Jermendy, Á. L., Panajotu, A., **Suhai, I. F.**, Drobni, Z. D., Karády, J., Tárnoki, Á. D., Tárnoki, D. L., Voros, S., Merkely, B., & Maurovich-Horvat, P. Effect of genetic and environmental influences on hepatic steatosis: A classical twin study based on computed tomography, Imaging, 12(1), 15-20. (2020)

31. Orbán G, Dohy Z, **Suhai FI**, Nagy AI, Salló Z, Boga M, Kiss M, Kunze K, Neji R, Botnar R, Prieto C, Gellér L, Merkely B, Vágó H, Szegedi N. Use of a new non-contrast-enhanced BOOST cardiac MR sequence before electrical cardioversion or ablation of atrial fibrillation-a pilot study. Front Cardiovasc Med. 2023 Jun 16;10:1177347.

32. Mihály Zsuzsanna, László Hidi, **Ferenc Suhai**, Zsófia Tarcza, Balázs Nemes, Péter Sótonyi. Nyaki verőér atípusos, fokális, fibromuscularis dysplasiájának képalkotó diagnosztikai nehézségei MAGYAR RADIOLÓGIA 2020; 94 : 1-2 pp. 70-74.

33. Vágó H , Tóth A , Czimbalmos Cs , **Suhai FI** , Kecskés K , Heltai K , Zima E , Bárczi Gy , Simor T , Becker D , Merkely B. Culprit lézió nélküli ST-elevációs miokardiális infarktus differenciáldiagnosztikája szív mágneses rezonanciavizsgálat segítségével
Cardiologia Hungarica 2014; 44:300-305.

34. **Suhai Ferenc Imre**, Sax Balázs, Assabiny Alexandra, Király Ákos, Czimbalmos Csilla, Csécs Ibolya, Kovács Attila, Latakos Bálint, Németh Endre, Becker Dávid, Szabolcs Zoltán, Hubay Márta, Merkely Béla, Vágó Hajnalka. A szív MR-vizsgálat szerepe kevert típusú (humorális és celluláris) kardiális allograft rejekció esetén. Cardiologia Hungarica 2018; 48:44-51.

35. Juhász G, Csőre J, **Suhai FI**, Gyánó M, Pataki Á, Vecsey-Nagy M, Pál D, Fontanini DM, Bérczi Á, Csobay-Novák C. A kontrasztanyag nélküli mágnesesrezonancia-angiográfia diagnosztikus teljesítménye alsó végtagi verőérbetegekben. Orv Hetil. 2022 Nov 6;163(45):1782-1788.

36. Hidi L, Csobay-Novák C, Juhász V, **Suhai F**, Szeberin Z, Sótonyi P. Postdissectiós aortaaneurysma endovascularis kezelése „candy-plug" technikával perzisztáló állumen esetén. Orv Hetil. 2020 Mar;161 (11):437-439.

37. Csécs Ibolya, Czimbalmos Csilla, Tóth Attila, Kiss Orsolya, Komka Zsolt, Bárczi György, Kováts Tímea, **Suhai Ferenc Imre**, Sydó Nóra, Simor Tamás , Gellér László, Becker Dávid, Merkely Béla, Vágó Hajnalka. Sportszív vagy strukturális szívizombetegség? Szív mágneses rezonanciás vizsgálat diagnosztikus szerepe sportolóknál strukturális szívbetegség gyanúja esetén. Cardiologia Hungarica 2017; 47:10-17.

38. Kádár Krisztina, Csőre Judit, Liptai Csilla, Tóth Attila, Kovács Attila, Molnár Levente, **Suhai Imre**, Assabiny Alexandra, Kuthi Luca, Édes István, Kertész

Attila Béla, Merkely Béla, Hartyánszky István. Kawasaki-betegség gyermekkortól a felnőttkorig. Multimodális képalkotók szerepe a hosszú távú nyomonkövetésben. Cardiologia Hungarica 2017; 47:243-249.

39. Borbola József, Sári Csaba, Som Zoltán, **Suhai Ferenc**, Csepregi András. Miért érdemes a Fradinak szurkolni a Groupama Arénában? Cardiologia Hungarica 2020; 50: 444–450.

40. Dohy Zsófia, Csécs Ibolya, Czimbalmos Csilla, **Suhai, Ferenc Imre**, Tóth, Attila, Szabó Liliána, Pozsonyi Zoltán, Simor Tamás, Merkely Béla, Vágó, Hajnalka. Balkamra-hipertrófiával, illetve megnövekedett falvastagsággal járó cardiomyopathiák szív mágneses rezonanciás jellegzetességei. Cardiologia Hungarica 2018; 48: 390-396.

41. A szív mágneses rezonanciás vizsgálatának szerepe lezajlott COVID-19-fertőzést követően Szabó Liliána, Juhász Vencel1, Dohy Zsófia, Hirschberg Kristóf, Czimbalmos Csilla, Tóth Attila, **Suhai Ferenc Imre**, Merkely Béla, Vágó Hajnalka
Cardiologia Hungarica 2021; 51: 18–22.Hirschberg Kristóf, Dohy Zsófia, Tóth Attila, Szabó Liliána, Czimbalmos Csilla, Finster Marius, **Suhai Ferenc**, Merkely Béla , Vágó Hajnalka.

42. A mappingtechnikák által nyújtott lehetőségek a szív-MR-vizsgálatok során: indikációk, diagnosztikus érték, limitációk és centrumunk kezdeti tapasztalatai Cardiologia Hungarica 2020; 50: 45–53.

10. Acknowledgements

parents for their enormous support during school and university years and far above. I acknowledge your limitless love and sacrifices.

I would like to express my heartfelt gratitude to my father for his invaluable guidance and unwavering support in directing me towards a scientific career. His influence and encouragement have played a crucial role in shaping my aspirations and achievements in the field of science.

 I am especially grateful to my wife, Nóra Éva Balogh whose continuous incentive and unrelenting love and patience helped me overcome one of the most difficult periods of my life so far. For you, I am eternally grateful.

11. Supplementary data

Supplement Table 1. Results of repeated measures analysis of variance on effects of sex, age and ischemic lesion volumen on diffusion tensor imaging metric changes

Repeated measures modell covariants: (Intercept), Sex female, Age, ILV group I, ILV group II		
BODY OF CORPUS CALLOSUM		
FA		
	F	p-value[*]
(Intercept):Time	1,0178	0,3164
Sex:Time	0,1784	0,6740
Age:Time	1,2683	0,2638
ILV group:Time	1,2427	0,2947
Error (Time)	1,0000	0,5000
Post hoc analysis (ILV group):		p-value[**]
I - II		0,9991
I - III		0,9836
II - III		0,9785
MD		
	F	p-value[*]
(Intercept):Time	0,0253	0,8742
Sex:Time	**5,2154**	**0,0254**
Age:Time	0,1947	0,6603

ILV_group:Time	**5,7180**	**0,0050**
Error (Time)	1,0000	0,5000
Post hoc analysis (ILV group):		p-value**
I - II		0,7509
I - III		0,0457
II - III		0,2601

AD		
	F	p-value*
(Intercept):Time	0,5819	0,4481
Sex:Time	**7,8653**	**0,0065**
Age:Time	1,5269	0,2206
ILV_group:Time	**5,8505**	**0,0045**
Error (Time)	1,0000	0,5000
Post hoc analysis (ILV group):		p-value**
I - II		0,6973
I - III		0,0183
II - III		0,1662

RD		
	F	p-value*
(Intercept):Time	0,0380	0,8461

Sex:Time	2,8593	0,0952
Age:Time	0,0030	0,9562
ILV_group:Time	**4,2827**	**0,0175**
Error (Time)	1,0000	0,5000
Post hoc analysis (ILV group):		p-value**
I - II		0,8963
I - III		0,3167
II - III		0,6183

CINGULATE GYRUS RIGHT

FA

	F	p-value*
(Intercept):Time	0,1624	0,6881
Sex:Time	2,8449	0,0960
Age:Time	0,0979	0,7553
ILV_group:Time	1,1007	0,3382
Error (Time)	1,0000	0,5000
Post hoc analysis (ILV group):		p-value**
I - II		0,6935
I - III		0,7418
II - III		0,9960

MD		
	F	p-value[*]
(Intercept):Time	1,0753	0,3032
Sex:Time	**9,1228**	**0,0035**
Age:Time	0,5434	0,4634
ILV_group:Time	1,1831	0,3122
Error(Time)	1,0000	0,5000
Post hoc analysis (ILV group):		p-value[**]
I - II		0,5721
I - III		0,3976
II - III		0,0832
AD		
	F	p-value[*]
(Intercept):Time	0,8880	0,3492
Sex:Time	**16,7079**	**0,0001**
Age:Time	0,5556	0,4585
ILV_group:Time	2,9204	0,0603
Error (Time)	1,0000	0,5000
Post hoc analysis (ILV group):		p-value[**]
I - II		0,3155

I - III		0,9565
II - III		0,2332
	RD	
	F	p-value*
(Intercept):Time	0,3923	0,5330
Sex:Time	0,5624	0,4557
Age:Time	0,1481	0,7015
ILV_group:Time	0,6144	0,5438
Error (Time)	1,0000	0,5000
Post hoc analysis (ILV group):		p-value**
I - II		0,9925
I - III		0,3557
II - III		0,4707
CINGULATE GYRUS LEFT		
	FA	
	F	p-value*
(Intercept):Time	3,9937	0,0494
Sex:Time	2,6541	0,1076
Age:Time	3,6973	0,0585
ILV_group:Time	0,4648	0,6301
Error (Time)	1,0000	0,5000

Post hoc analysis (ILV group):		p-value[**]
I - II		0,9609
I - III		0,8884
II - III		0,9827
MD		
	F	p-value[*]
(Intercept):Time	0,0001	0,9923
Sex:Time	3,2490	0,0757
Age:Time	0,0974	0,7559
ILV_group:Time	0,9744	0,3823
Error (Time)	1,0000	0,5000
Post hoc analysis (ILV group):		p-value[**]
I - II		0,3121
I - III		0,1790
II - III		**0,0087**
AD		
	F	p-value[*]
(Intercept):Time	1,4348	0,2349
Sex:Time	**7,9737**	**0,0062**
Age:Time	1,9016	0,1722

ILV_group:Time	1,6466	0,1999
Error (Time)	1,0000	0,5000
Post hoc analysis (ILV group):		p-value[**]
I - II		0,4454
I - III		0,8015
II - III		0,1999

RD		
	F	p-value[*]
(Intercept):Time	1,1942	0,2781
Sex:Time	0,0141	0,9059
Age:Time	0,7101	0,4022
ILV_group:Time	0,2506	0,7790
Error (Time)	1,0000	0,5000
Post hoc analysis (ILV group):		p-value[**]
I - II		0,8536
I - III		0,2971
II - III		0,1447

PARAHIPPOCAMPAL CINGULUM RIGHT		
FA		

	F	p-value[*]
(Intercept):Time	0,0008	0,9773
Sex:Time	0,8925	0,3480
Age:Time	0,0031	0,9558
ILV_group:Time	0,3322	0,7184
Error (Time)	1,0000	0,5000
Post hoc analysis (ILV group):		p-value[**]
I - II		0,7997
I - III		0,7695
II - III		0,9991
MD		
	F	p-value[*]
(Intercept):Time	1,7424	0,1910
Sex:Time	0,1480	0,7015
Age:Time	2,2941	0,1342
ILV_group:Time	0,1328	0,8758
Error (Time)	1,0000	0,5000
Post hoc analysis (ILV group):		p-value[**]
I - II		0,6278
I - III		0,3976

II - III		0,9373

AD		
	F	p-value[*]
(Intercept):Time	2,0353	0,1580
Sex:Time	0,9604	0,3304
Age:Time	2,7919	0,0991
ILV_group:Time	0,0755	0,9273
Error (Time)	1,0000	0,5000
Post hoc analysis (ILV group):		p-value[**]
I - II		0,8251
I - III		0,6110
II - III		0,9433
RD		
	F	p-value[*]
(Intercept):Time	1,3039	0,2573
Sex:Time	0,0001	0,9911
Age:Time	1,6630	0,2013
ILV_group:Time	0,1850	0,8315
Error (Time)	1,0000	0,5000

Post hoc analysis (ILV group):		p-value[**]
I - II		0,6372
I - III		0,4488
II - III		0,9597

PARAHIPPOCAMPAL CINGULUM LEFT

FA

	F	p-value[*]
(Intercept):Time	1,9876	0,1629
Sex:Time	0,4981	0,4826
Age:Time	2,1288	0,1489
ILV_group:Time	2,7031	0,0738
Error (Time)	1,0000	0,5000
	1,9876	0,1629

Post hoc analysis (ILV group):		p-value[**]
I - II		0,9767
I - III		0,6799
II -III		0,5932

MD

	F	p-value[*]
(Intercept):Time	0,7559	0,3875
Sex:Time	2,8307	0,0968

Age:Time	0,6430	0,4253
ILV_group:Time	0,9344	0,3975
Error (Time)	1,0000	0,5000
Post hoc analysis:		
ILV_group		p-value[**]
I - II		0,9202
I - III		0,9990
II -III		0,9128
AD		
	F	p-value[*]
(Intercept):Time	0,0464	0,8301
Sex:Time	1,2850	0,2607
Age:Time	0,0127	0,9105
ILV_group:Time	0,0984	0,9064
Error (Time)	1,0000	0,5000
Post hoc analysis (ILV group):		p-value[**]
I - II		0,9859
I - III		0,9405
II - III		0,9862
RD		

	F	p-value[*]
(Intercept):Time	1,4764	0,2283
Sex:Time	3,3644	0,0708
Age:Time	1,3985	0,2409
ILV_group:Time	1,7538	0,1804
Error (Time)	1,0000	0,5000
Post hoc analysis (ILV group):		p-value[**]
I - II		0,8887
I - III		0,9382
II - III		0,7316

GENU OF CORPUS CALLOSUM

FA

	F	p-value[*]
(Intercept):Time	0,5981	0,4418
Sex:Time	0,4440	0,5073
Age:Time	0,8617	0,3564
ILV_group:Time	1,4027	0,2526
Error (Time)	1,0000	0,5000
Post hoc analysis (ILV group):		p-value[**]
I - II		0,4764

I - III		0,6600
II - III		0,9542

MD		
	F	p-value[*]
(Intercept):Time	0,1937	0,6612
Sex:Time	1,4284	0,2359
Age:Time	0,3453	0,5586
ILV_group:Time	0,6402	0,5302
Error (Time)	1,0000	0,5000
Post hoc analysis (ILV group):		p-value[**]
I - II		0,9115
I - III		0,8223
II - III		0,6146

AD		
	F	p-value[*]
(Intercept):Time	0,6010	0,4407
Sex:Time	1,9831	0,1634
Age:Time	1,1466	0,2878
ILV_group:Time	1,0326	0,3613
Error (Time)	1,0000	0,5000

Post hoc analysis (ILV group):		p-value[**]
ILV_group		p-value[**]
I - II		0,8927
I - III		0,4006
II -III		0,7162
	RD	
	F	p-value[*]
(Intercept):Time	0,0253	0,8739
Sex:Time	0,7564	0,3873
Age:Time	0,0361	0,8498
ILV_group:Time	0,8269	0,4415
Error (Time)	1,0000	0,5000
Post hoc analysis (ILV group):		p-value[**]
I - II		0,5728
I - III		0,9697
II - III		0,7437
SPLENIUM OF CORPUS CALLOSUM		
	FA	
	F	p-value[*]
(Intercept):Time	0,2723	0,6034
Sex:Time	1,9443	0,1675

Age:Time	0,6844	0,4108
ILV_group:Time	0,0519	0,9495
Error (Time)	1,0000	0,5000
Post hoc analysis (ILV group):		p-value[**]
I - II		0,9445
I - III		0,8838
II -III		0,7372

MD		
	F	p-value[*]
(Intercept):Time	0,7679	0,3838
Sex:Time	0,0352	0,8518
Age:Time	0,7272	0,3966
ILV_group:Time	0,4999	0,6087
Error (Time)	1,0000	0,5000
Post hoc analysis (ILV group):		p-value[**]
I - II		0,9811
I - III		0,1063
II -III		0,0986

AD		
	F	p-value[*]

(Intercept):Time	2,8627	0,0950
Sex:Time	0,2242	0,6373
Age:Time	3,7012	0,0583
ILV_group:Time	1,5172	0,2263
Error(Time)	1,0000	0,5000
Post hoc analysis (ILV group):		p-value[**]
I - II		0,9788
I - III		0,0462
II -III		0,1023
RD		
	F	p-value[*]
(Intercept):Time	0,0999	0,7528
Sex:Time	0,2744	0,6020
Age:Time	0,0244	0,8763
ILV_group:Time	0,1275	0,8805
Error (Time)	1,0000	0,5000
Post hoc analysis (ILV group):		p-value[**]
I - II		0,9183
I - III		0,3766
II -III		0,2427

AD= axial diffusivity; F= F-statistic; FA= fractional anisotropy; FU= follow up; ILV= ischemic lesion volumen; MD= mean diffusivity; RD= radial diffusivity.

*P-values with Greenhouse-Geisser, Huynh-Feldt and lower bound adjustment (not included) were similar to p-values for the corresponding F-statistics in all categories.
**Bonferroni-corrected p-values significant if <0.0167.

Supplement Table 2. Procedural characteristics of patients with bicuspid and tricuspid valve

Patient data (n=113)	Bicuspid (n=15)	Tricuspid (n=98)	p
Aortic valve calcium score	*4913 ±2800*	*3078 ±1668*	*<0.001*
Ischemic load (mm^3)	4789 ± 21800	4086 ± 17450	0.95
Access route (TF vs. TS vs. TC), n (%)	*12 (80.0) vs. 3 (20.0)*	*93 (94.9) vs. 5 (5.1)*	*0.04*
Pre-dilatation, n (%)	3 (20.0)	12 (12.2)	0.41
CoreValve vs. Portico, n (%)	13 (86.7) vs. 2 (13.3)	71 (72.4) vs. 27 (27.6)	0.24
Malposition/Migration, n (%)	0 (0.0)	3 (3.1)	1.00
Post-dilatation, n (%)	14 (93.3)	75 (76.5)	0.14
Stroke (%)	2 (13.3)	4 (4.1)	0.14
Vascular complications/bleeding, n (%)			
Minor (according to VARC-3 criteria)	2 (13.3)	15 (15.3)	0.84
Major (according to VARC-3 criteria)	2 (13.3)	8 (8.2)	0.51

TF: Transfemoral; TS: Transsubclavian; TC: Transcarotid; VARC-3, Valve Academic Research Consortium.

Continuous variables are described as mean ± SD, whereas categorical variables are represented as frequencies and percentage.